University of Massachusetts Medical School
eScholarship@UMMS

GSBS Dissertations and Theses | Graduate School of Biomedical Sciences

2016-08-03

Roles of the Mother Centriole Appendage Protein Cenexin in Microtubule Organization during Cell Migration and Cell Division: A Dissertation

Hui-Fang Hung
University of Massachusetts Medical School

Let us know how access to this document benefits you.
Follow this and additional works at: https://escholarship.umassmed.edu/gsbs_diss

 Part of the Cell Biology Commons, and the Cellular and Molecular Physiology Commons

Repository Citation
Hung H. (2016). Roles of the Mother Centriole Appendage Protein Cenexin in Microtubule Organization during Cell Migration and Cell Division: A Dissertation. GSBS Dissertations and Theses. https://doi.org/10.13028/M2QC73. Retrieved from https://escholarship.umassmed.edu/gsbs_diss/842

This material is brought to you by eScholarship@UMMS. It has been accepted for inclusion in GSBS Dissertations and Theses by an authorized administrator of eScholarship@UMMS. For more information, please contact Lisa.Palmer@umassmed.edu.

ROLES OF THE MOTHER CENTRIOLE APPENDAGE PROTEIN CENEXIN IN MICROTUBULE ORGANIZATION DURING CELL MIGRATION AND CELL DIVISION

A Dissertation Presented

By

HUI-FANG HUNG

Submitted to the Faculty of the

University of Massachusetts Graduate School of Biomedical Sciences, Worcester

In partial fulfillment of the requirements for the degree of

DOCTOR OF PHILOSOPHY

AUGUST 3rd, 2016

INTERDISCIPLINARY GRADUATE PROGRAM

ROLES OF THE MOTHER CENTRIOLE APPENDAGE PROTEIN CENEXIN IN MICROTUBULE ORGANIZATION DURING CELL MIGRATION AND CELL DIVISION

A Dissertation Presented
By
Hui-Fang Hung

The signatures of the Dissertation Defense Committee signify completion and approval as to style and content of the Dissertation

Stephen Doxsey, PhD., Thesis Advisor

Yicktung Tony Ip, PhD., Member of Committee

Thomas Maresca, PhD., Member of Committee

Dannel McCollum, PhD., Member of Committee

William Theurkauf, PhD., Member of Committee

The signature of the Chair of the Committee signifies that the written dissertation meets the requirements of the Dissertation Committee

David Lambright, PhD., Chair of Committee

The signature of the Dean of the Graduate School of Biomedical Sciences signifies that the student has met all graduation requirements of the school

Anthony Carruthers, PhD.,
Dean of the Graduate School of Biomedical Sciences

Interdisciplinary Graduate Program

August 3rd, 2016

ABSTRACT

Epithelial cells are necessary building blocks of the organs they line. Their apical-basolateral polarity, characterized by an asymmetric distribution of cell components along their apical-basal axis, is a requirement for normal organ function. Although the centrosome, also known as the microtubule organizing center, is important in establishing cell polarity the mechanisms through which it achieves this remain unclear. It has been suggested that the centrosome influences cell polarity through microtubule cytoskeleton organization and endosome trafficking. In the first chapter of this thesis, I summarize the current understanding of the mechanisms regulating cell polarity and review evidence for the role of centrosomes in this process.

In the second chapter, I examine the roles of the mother centriole appendages in cell polarity during cell migration and cell division. Interestingly, the subdistal appendages, but not the distal appendages, are essential in both processes, a role they achieve through organizing centrosomal microtubules. Depletion of subdistal appendages disrupts microtubule organization at the centrosome and hence, affects microtubule stability. These microtubule defects affect centrosome reorientation and spindle orientation during cell migration and division, respectively. In addition, depletion of subdistal appendages affects the localization and dynamics of apical polarity proteins in relation to microtubule stability and endosome recycling. Taken together, our results suggest the mother centriole subdistal appendages play an essential role in regulating cell polarity. A discussion of the significance of these results is included in chapter three.

TABLE OF CONTENTS

LIST OF FIGURES

Chapter I

Chapter II

Appendix

COPYRIGHTED MATERIALS

Chapter II has appeared in a separate publication.

Hung, H.-F., Hehnly, H., Doxsey, S. (2016). The mother centriole appendage protein cenexin modulates lumen formation through spindle orientation. Curr Biol. *26*, 793-801.

PREFACE

With minor alternations, part of this dissertation has been published in the following manuscripts:

Chapter I is in preparation for publication:

Hung, H.-F., and Doxsey, S. The mother centriole appendage protein cenexin.

Chapter II has been published previously:

Hung, H.-F., Hehnly, H., Doxsey, S. (2016). The mother centriole appendage protein cenexin modulates lumen formation through spindle orientation. Curr Biol. *26*, 793-801.

In addition, I assisted with the research presented in the following published works during my PhD studies:

Vertii, A., **Hung, H.-F.**, Hehnly, H., and Doxsey, S. (2016). Human basal body basics. Cilia *5*, 1–7.

Hung, H.-F., Hehnly, H., Doxsey, S. (2015) Methods to analyze novel liaisons between endosomes and centrosomes. Methods Cell Biol. 130, 47-58.

Chen, C.-T., Hehnly, H., Yu, Q., Farkas, D., Zheng, G., Redick, S.D., **Hung, H.-F.**, Samtani, R., Jurczyk, A., Akbarian, S., et al. (2014). A Unique Set of Centrosome Proteins Requires Pericentrin for Spindle-Pole Localization and Spindle Orientation. Curr. Biol. 24, 2327–2334.

Hehnly, H., **Hung, H.-F.**, and Doxsey, S. (2013). One among many: ODF2 isoform 9, a.k.a. Cenexin-1, is required for ciliogenesis. Cell Cycle 12, 1021.

Hung, H.-F., Hehnly, H, Doxsey, S. (2012) Multiplying madly: Deacetylases take charge of centrosome duplication and amplification. Cell Cycle 11, 4304.

CHAPTER I

GENERAL INTRODUCTION

Organization of epithelial cell polarity and de novo lumen formation.

The epithelial cell is a fundamental cell type in mammals, that lines skin, glands and organs including the breast, intestine and kidney. These cells are highly polarized with discrete apical and basolateral polarity featured with asymmetric distribution of membrane, polarity proteins, and organelles (Rodriguez-Boulan and Macara, 2014). This polarity is important in maintaining tissue function and structure, and also for controlling cell differentiation and cell proliferation. Disruption of the apical-basolateral polarity can generate epithelial tumors, which make up more than 90% of solid tumors in humans (Bryant and Mostov, 2008; Martin-belmonte and Perez-moreno, 2011; McCaffrey and Macara, 2011; Muthuswamy and Xue, 2012).

An interesting and fundamental question is how do cells establish and maintain cell polarity. Furthermore, how is cell polarity involved in tissue structure and function. Within the last couple of decades, three-dimensional (3D) culture of epithelial cells has become a powerful tool to study cell polarity and tumorigenesis (Schmeichel and Bissell, 2003). Compared to classic 2D culture, 3D culture better recapitulates the growth environment *in vivo*. Most of the primary cells or established cell lines from epithelial organs (breast, intestine and kidney) can grow in suspension with extracellular matrix (ECM) and form acinar or tubular structures with a monolayer of cells surrounding a single hollow lumen, which resembles the basic function and tissue structure of the epithelium in animals. Epithelial cells of 3D-cultured acini are highly polarized with the apical surface toward the lumen and the basal surface in contact with ECM. The distinct localization of polarity

proteins is the key to maintain cell polarity and also direct control cell proliferation and tissue structure.

Polarized membrane transport directly participate in the delivery and recycling of polarity proteins, and Rab protein is the master regulator of this process (Blasky et al., 2015; Rodriguez-Boulan and Macara, 2014; Stenmark, 2009). The Rab family proteins are conserved small GTPases that switch between the active GTP-bound form and the inactive GDP-bound form to coordinate membrane trafficking in eukaryotic cells. There are more than 60 Rab proteins in humans, and these Rabs localize and associate with distinct intracellular membranes and cargos to direct vesicle trafficking (Blasky et al., 2015). For example, Rab8 assists the apical (Sato et al., 2007, 2014) and basolateral (Ang et al., 2003; Henry and Sheff, 2008) membrane delivery of newly synthesized polarity proteins through the trans-Golgi network (TGN) to the plasma membrane. Apical and basolateral localized proteins then can be endocytosed and recycled back to the plasma membrane or sent to the lysosome for degradation.

In addition, the specific localization of polarity proteins is required for building and expanding a single symmetric lumen (Overeem et al., 2015; Rodríguez-Fraticelli et al., 2011). During lumen formation starting from one single cell, the orientation of cell division determines the position of the apical lumen. During symmetric lumen expansion though cell division, the basolateral membrane localized NuMA/LGN/Gαi complex orients mitotic spindles parallel to the apical lumen in the manner dependent on the apical localized PAR/aPKC complex. Disruption of either apical or basolateral protein complex leads to

multiple lumen formation by causing spindle misorientaion (Durgan et al., 2011; Hao et al., 2010; Jaffe et al., 2008; Zheng et al., 2010).

The centrosome as a microtubule-organizing center (MTOC) mediates organelle positioning and cell polarity.

The centrosome, also known as the microtubule-organizing center (MTOC), is essential for multiple cellular functions, including cell polarization and cell division which are important for lumen formation. Through the microtubule array that radiates from the centrosome, centrosomes organize the localization of the Golgi apparatus (Sütterlin and Colanzi, 2010) and also directly control the trafficking of recycling endosomes (Gromley et al., 2005; Hehnly et al., 2012; Ullrich et al., 1996), thus contributing to cell polarization. Importantly, the correct positioning of the centrosome itself is also essential for cell polarization. In many cell types, including fibroblasts and epithelial cells, centrosomes localize near the center of the cell (Elric and Etienne-Manneville, 2014; Tang and Marshall, 2012) through pull/push forces generated by the microtubule array emanated from centrosomes against the plasma membrane (Holy et al., 1997).

A good example and model of centrosome position in regulating cell polarity is the reorientation of the centrosome-nucleus axis during cell migration. After migration is induced, the centrosome stays at the cell centroid while the nucleus moves backward with actin flow (Luxton et al., 2011). This centrosome reorientation is essential for enabling cells to establish a front-rear polarity with Golgi and apical polarity proteins, such as PAR and aPKC, localizing toward the leading edge. Microtubule dynamics and the microtubule

motor dynein are required for this centrosome centering process (Luxton and Gundersen, 2011; Magdalena et al., 2003; Salaycik et al., 2005; Schmoranzer et al., 2009; Wu et al., 2011). In addition, disruption of centrosome integrity by laser ablation also affects front-rear cell polarization, directional migration and cell motility (Wakida et al., 2010). Moreover, during cell migration, microtubules at the centrosome are selectively stabilized toward the leading edge through a Rho-dependent pathway (Cook et al., 1998; Palazzo et al., 2001; Salaycik et al., 2005). These results suggest that the centrosome can position itself through organizing microtubules and mediating microtubule stability.

Centrosome structure and possible centrosome components that contribute to microtubule organization and cell polarity.

The centrosome is composed of a pair of centrioles embedded in pericentriolar material (PCM). One of the centriole, which is called the mother centriole, possesses two sets of appendages (the distal and subdistal appendages) on its distal end, while the other centriole is naked and is called the daughter centriole (Bornens, 2012; Doxsey, 2001). During cell division, each of the two centrioles will be used as a template for centrosome duplication from S to G2 phase. At G2/M transition, the daughter centriole from the old centrosome acquires appendage proteins, which is the hallmark of centrosome maturation (Graser et al., 2007; Kong et al., 2014; Lange and Gull, 1995). These two centrosomes then serve as the two poles of a mitotic spindle, and will be distributed to each daughter cell later on (Figure 1.1; Bettencourt-Dias and Glover, 2007; Bornens, 2012; Fırat-karalar and Stearns, 2014). In arresting cells, the centrosome serves as the basal body for a cilium, and

the mother centriole appendages are essential for cilium formation and function (Chang et al., 2013; Graser et al., 2007; Vertii et al., 2016). However, the role of these appendages outside of cilia is poorly understood.

There is evidence suggesting that mother centriole appendages are specifically involved in the establishment or maintenance of cell polarity. First of all, the mother centriole (but not the daughter centriole) anchors microtubules and is involved in centrosome centering (Piel et al., 2000). Moreover, subdistal appendages have been shown to directly anchor microtubules at the mother centriole using electron microscopy (EM) (Bornens, 2002, 2012). This was further validated using high resolution structured illumination microscopy (SIM) that showed microtubules are preferentially attached to the subdistal appendage structural protein cenexin (Figure 1.2). Ninein, which localized at the proximal ends of centrioles and the mother centriole appendages, directs microtubules nucleated in PCM by γ-tubulin ring complex (γTuRC) and related γ-tubulin complex (Kollman et al., 2011) to the mother centriole subdistal appendages (Delgehyr et al., 2005; Mogensen et al., 2000). Depletion of subdistal appendage proteins ninein, CEP170 and cenexin disrupts microtubule array organization at the centrosome without affecting the localization of PCM proteins and microtubule nucleation activity (Delgehyr et al., 2005; Guarguaglini et al., 2005; Ishikawa et al., 2005; Tateishi et al., 2013). Based on the role of subdistal appendages in anchoring and organizing microtubule arrays, these appendages may contribute to cell polarization by controlling centrosome positioning.

Secondly, both the distal and subdistal appendages of the mother centriole directly interact with recycling endosome components and participate in ciliary vesicle formation during ciliogenesis (Chang et al., 2013; Hehnly et al., 2012; Schmidt et al., 2012; Westlake et al., 2011). For example, the distal appendage protein, CEP164, binds to Rab8 and Rabin8, which is the guanine nucleotide exchange factor (GEF) for Rab8. Rab8 localizes to centrosomes in a manner dependent on the distal appendages and can be activated by Rabin8, which also localizes specifically at the distal appendages. Depletion of CEP164, which also disrupts distal appendages, affects Rab8 centrosomal localization and leads to accumulation of vesicles around the centrosome (Graser et al., 2007; Schmidt et al., 2012), which suggests that Rab8 at the distal appendages participates directly in pericentriolar endosome trafficking. The subdistal appendage protein, cenexin, also preferentially binds to the active form of Rab8 (Chang et al., 2013). Since Rab8 participates in apical and basolateral protein transport in epithelial cells (Ang et al., 2003; Henry and Sheff, 2008; Sato et al., 2007, 2014), the centrosomal localization of Rab8 may not only be essential for early ciliogenesis but also important for cell polarization.

In addition, the subdistal appendage acts as a hub for coordinating Rab11-dependent endosome trafficking in non-ciliated cells (Gromley et al., 2005; Hehnly et al., 2012; Ullrich et al., 1996). Cenexin is the fundamental structural protein of subdistal appendages, and depletion of cenexin disrupts the subdistal appendages (Chang et al., 2013; Ishikawa et al., 2005). Centriolin is another mother centriole subdistal appendage protein, and is required for the mother centriole localization of exocyst subunits (Sec6, Sec15, and Sec84) and the Rab11 GTPase activating protein (GAP) Evi5 (Dabbeekeh et

al., 2007; Faitar et al., 2005; Gromley et al., 2005; Hehnly et al., 2012). Interestingly, depletion of cenexin or centriolin have opposite effects on endosome recycling; depletion of centriolin increases the rate of recycling, while depletion of cenexin decreases the rate and causes accumulation of vesicles around the centrosome. Cenexin or the subdistal appendage preferentially binds to active Rab11, which is required for pericentriolar endosome trafficking. The Rab11 GAP Evi5, which localizes at mother subdistal appendages through centriolin, regulates Rab11 activity at the centrosome. Therefore, depletion of centriolin keeps active Rab11 at centrosomes and thus, increases endosome recycling (Hehnly et al., 2012).

The above results suggest that the mother centriole appendage, specifically the subdistal appendage, is the key centrosome component regulating cell polarization based on its roles in microtubule anchoring/organizing and pericentriolar endosome trafficking.

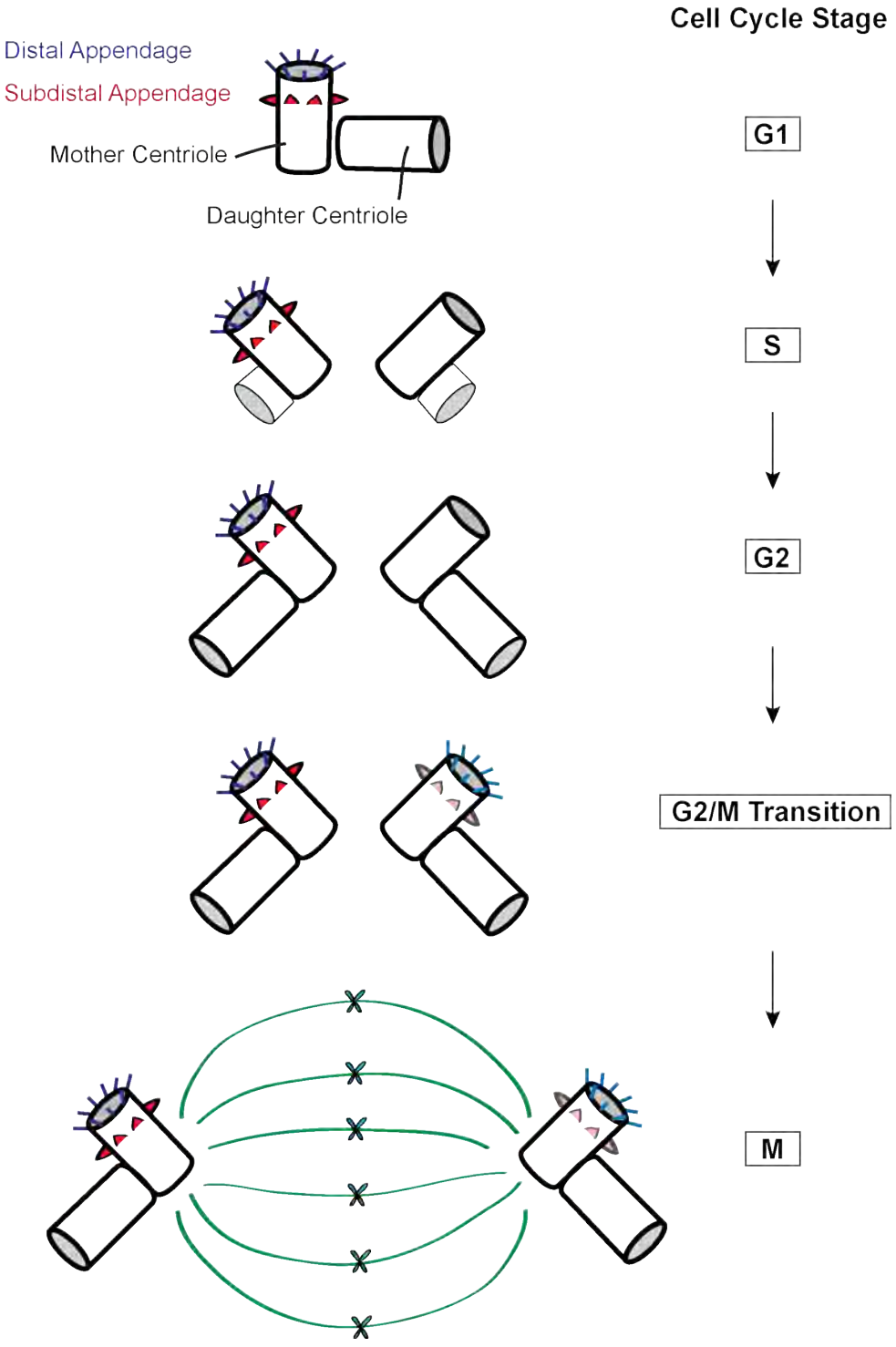

Figure 1.1 The centrosome cycle.

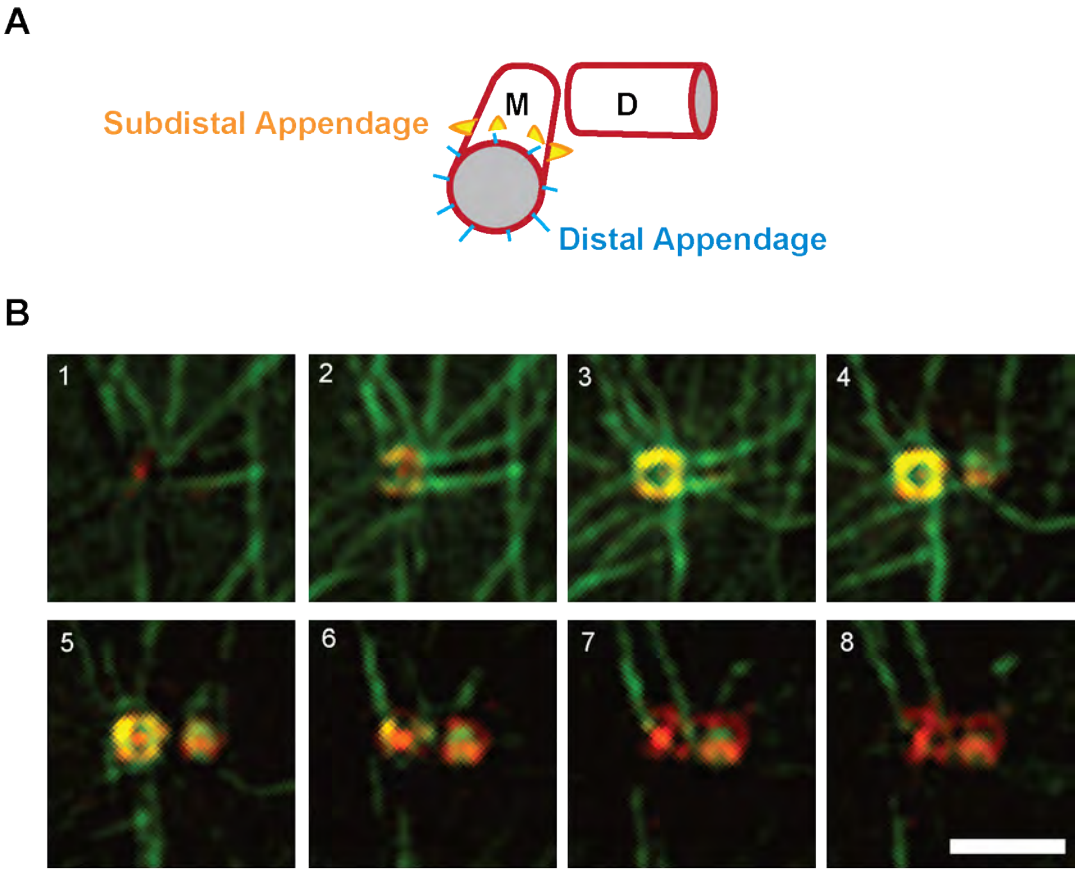

Figure 1.2 Microtubules anchor at the subdistal appendages.
(A) A model depicting the orientation of the centrosome in (B). The mother centriole is labeled as "M", and the daughter centriole is labeled as "D".
(B) Normal human fibroblasts were cultured on coverslips and prepared for immuno-fluorescence staining. Images were taken and processed using a DeltaVision OMX super-resolution microscope system. Images 1-8 show the microtubule organization at the centrosome with 0.125-μm interval. In images 3-4, microtubules (green) are specifically radiated from the subdistal appendage (yellow). The subdistal appendage (cenexin, light orange). Centrioles (γ-tubulin, red). Scale bar, 1 μm.

CHAPTER II

THE MOTHER CENTRIOLE APPENDAGE PROTEIN CENEXIN MODULATES LUMEN FORMATION THROUGH SPINDLE ORIENTATION

ABSTRACT

Establishing an apical-basal polarity axis is instrumental in the functional shaping of a solitary lumen within an acinus. By exploiting micropatterned slides, wound healing assays, and three-dimensional culture systems, we identified a mother centriole subdistal appendage protein, cenexin, as a critical player in symmetric lumen expansion through the control of microtubule organization. In this regard, cenexin was required for both centrosome positioning in interphase cells and proper spindle orientation during mitosis. In contrast, the essential mother centriole distal appendage protein, CEP164, did not play a role in either process, demonstrating the specificity of subdistal appendages for these events. Importantly, upon closer examination we found that cenexin depletion decreased astral microtubule length, disrupted astral microtubule minus-end organization and increased levels of the polarity protein, NuMA, at the cell cortex. Interestingly, spindle misorientation and NuMA mislocalization were reversed by treatment with a low-dose of the microtubule-stabilizing agent, taxol. Taken together, these results suggest that cenexin modulates microtubule organization and stability to mediate spindle orientation.

INTRODUCTION

In organs such as breast, kidney and intestine, polarized epithelial cells form acini, each with a single lumen (Figure 2.1, left) (Overeem et al., 2015). However, in epithelial pre-invasive carcinomas, disruption of apical-basal polarity leads to multiple ectopic lumina (Figure 2.1, right) (McCaffrey and Macara, 2011; Monteleon and D'Souza-Schorey, 2012). Thus, a better understanding of the molecular mechanism responsible for multiple lumina formation will provide insight into the origin and progression of epithelial diseases.

Formation of a solitary central lumen requires both regulated apical membrane/lumen establishment and subsequent symmetric lumen expansion (Overeem et al., 2015). Lumen generation requires a single epithelial cell to undergo the first cell division. After division, both mother and daughter cell centrosomes/spindle poles reorient to a position where the newly forming apical plasma membrane will emerge (Rodríguez-Fraticelli et al., 2012). In subsequent cell divisions, spindle orientation must be tightly regulated to complete apical domain formation at the center of a developing acinus (Overeem et al., 2015). More specifically, dividing cells must orient their mitotic spindles parallel to the apical lumen to symmetrically expand the already existing central lumen.

The molecular components that modulate spindle orientation involve proteins at mitotic spindle poles and polarity proteins at the lateral cell cortex. Many spindle pole proteins are involved in nucleating and anchoring microtubules. The polarity protein complex (NuMA/LGN/Gαi) is thought to capture astral microtubules at the lateral cell cortex

(Gillies and Cabernard, 2011; Kotak and Gönczy, 2013; Kotak et al., 2014; Zheng et al., 2010, 2013). However, the molecular interface between mitotic spindle poles, astral microtubules, and cortical capture of astral microtubules is poorly understood.

The centrosome is an essential contributor to cell polarity. In luminal epithelial cells, the centrosome is involved in polarity formation in two distinct ways: 1) during cell division it organizes and orients the mitotic spindle ensuring single lumen expansion (Jaffe et al., 2008), and 2) in interphase it repositions itself toward the apical membrane (Rodríguez-Fraticelli et al., 2012). More specifically, during mitosis the pericentriolar material proteins, pericentrin and CEP215, contribute to spindle orientation through their interaction with the mother centriole subdistal appendage proteins, centriolin and ninein (Chen et al., 2014). In interphase, the subdistal appendage protein, cenexin, anchors both centriolin and ninein to subdistal appendages (Gromley et al., 2003; Hehnly et al., 2012; Soung et al., 2009). Cenexin is also known to be important for the structural integrity of the subdistal appendages (Tanos et al., 2013). Thus, we hypothesize that these mother centriole specific substructures, and the molecular components associated with them (above), may play a role in spindle orientation and centrosome positioning. In this study, we test this hypothesis and compare results with an essential distal appendage component, CEP164 (Graser et al., 2007), to dissect the role of subdistal appendages versus distal appendages in lumen formation.

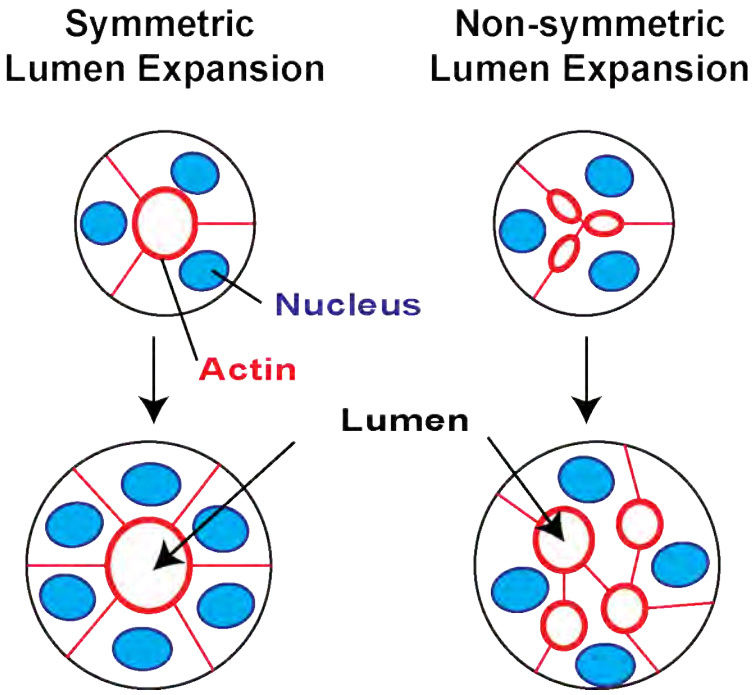

Figure 2.1 A schematic of the symmetric and non-symmetric lumen expansion.
A model depicting symmetric lumen expansion where acini expand around the central lumen (left), and non-symmetric lumen expansion where cells expand while creating multiple unorganized lumina (right).

RESULTS

The subdistal appendage protein, cenexin, but not the distal appendage protein, CEP164, is required for solitary lumen establishment.

To determine which appendage type was required for lumen formation, we created cell lines stably depleted of CEP164 (distal appendage protein) and cenexin (subdistal appendage protein) (Figure 2.2). Depletion of both was confirmed by loss of primary cilia (Figure 2.3) as shown previously (Chang et al., 2013; Graser et al., 2007; Hehnly et al., 2013). In addition, subdistal appendage proteins, centriolin (Gromley et al., 2003; Hehnly et al., 2012) and CEP128 (Jakobsen et al., 2011; Schrøder et al., 2012) were lost after cenexin depletion (Figure 2.4). Importantly cenexin depletion did not disrupt CEP164 localization to distal appendages, and CEP164 depletion had no effect on cenexin localization to subdistal appendages (Figure 2.5) (Schmidt et al., 2012; Tanos et al., 2013). This result demonstrated that cenexin depletion targeted subdistal appendages specifically.

Based on these findings, we tested lumen formation following depletion of CEP164 or cenexin (Figure 2.6). At early stages of acinus formation (acini with ≤5 cells), the majority of control cells (94%, GAPDH-depleted) formed acini with a single lumen. Similar results were obtained with CEP164-depleted cells (81%). In contrast, only 55% of cenexin-depleted cells formed acini with a single lumen. As acini expanded with multiple cell divisions (acini containing >5 cells), the percentage of acini with multiple lumina was low in control (27%) and CEP164-depleted cells (37%), compared to 60% in cenexin-depleted cells (Figure 2.6B and 2.6C). These findings suggest a role for the subdistal

appendage protein, cenexin, in symmetric lumen formation and expansion. Due to the significant increase of acini with multiple lumina in cenexin-depleted cells, we hypothesized that cenexin governs lumen formation by regulating centrosome positioning and spindle orientation during various stages of the cell cycle.

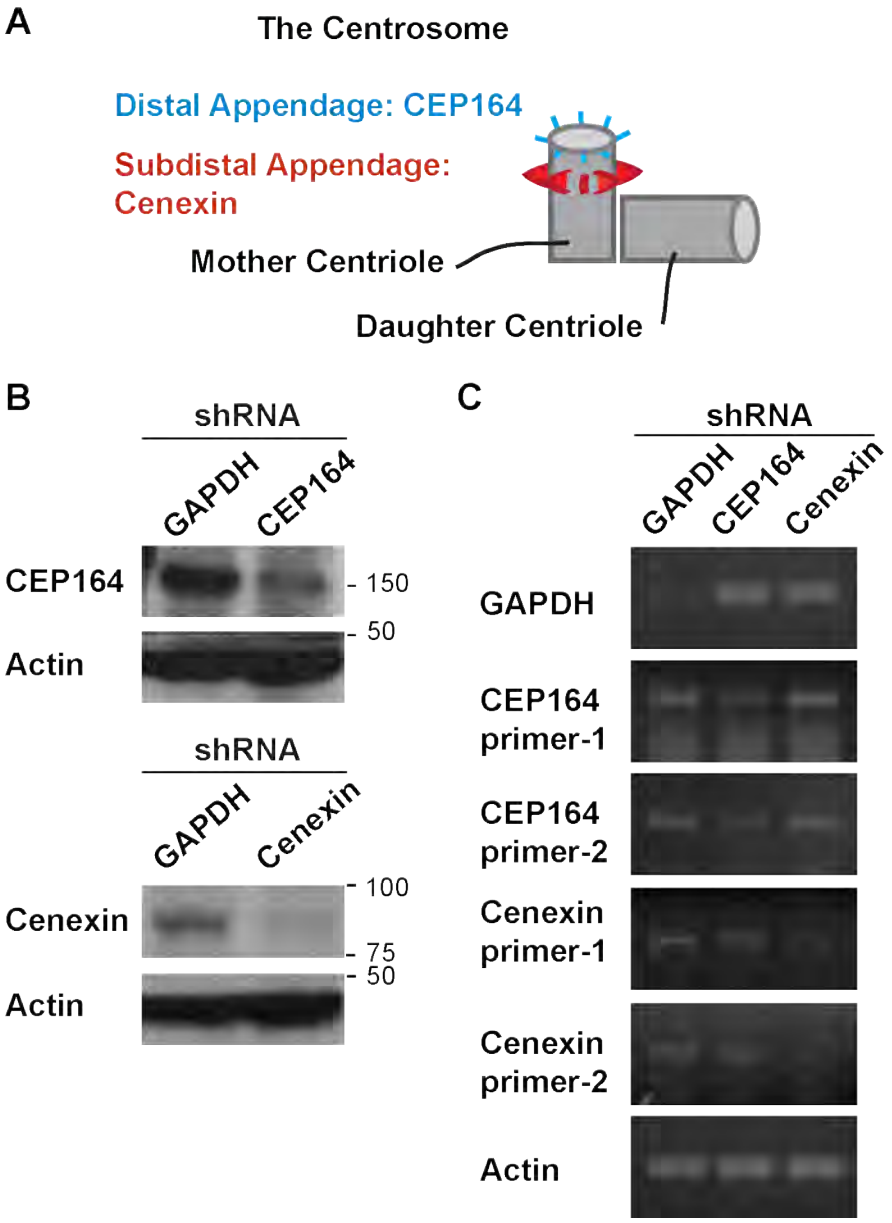

Figure 2.2 Creating cell lines depleted of distal or subdistal appendage proteins.
(A) A model depicting CEP164 localization to distal appendages (blue) and cenexin localization to subdistal appendages (red) on the mother centriole.
(B) Immunoblot analysis of U2OS cells treated with CEP164 shRNA (upper images) or cenexin shRNA (lower images), and compared to cells treated with control shRNA (GAPDH). Staining with antibodies to actin (loading control), and CEP164 (top) or cenexin (bottom).
(C) RT-PCR analysis showing CEP164 and cenexin gene expression in MDCK cells depleted of GAPDH (control), CEP164 or cenexin.

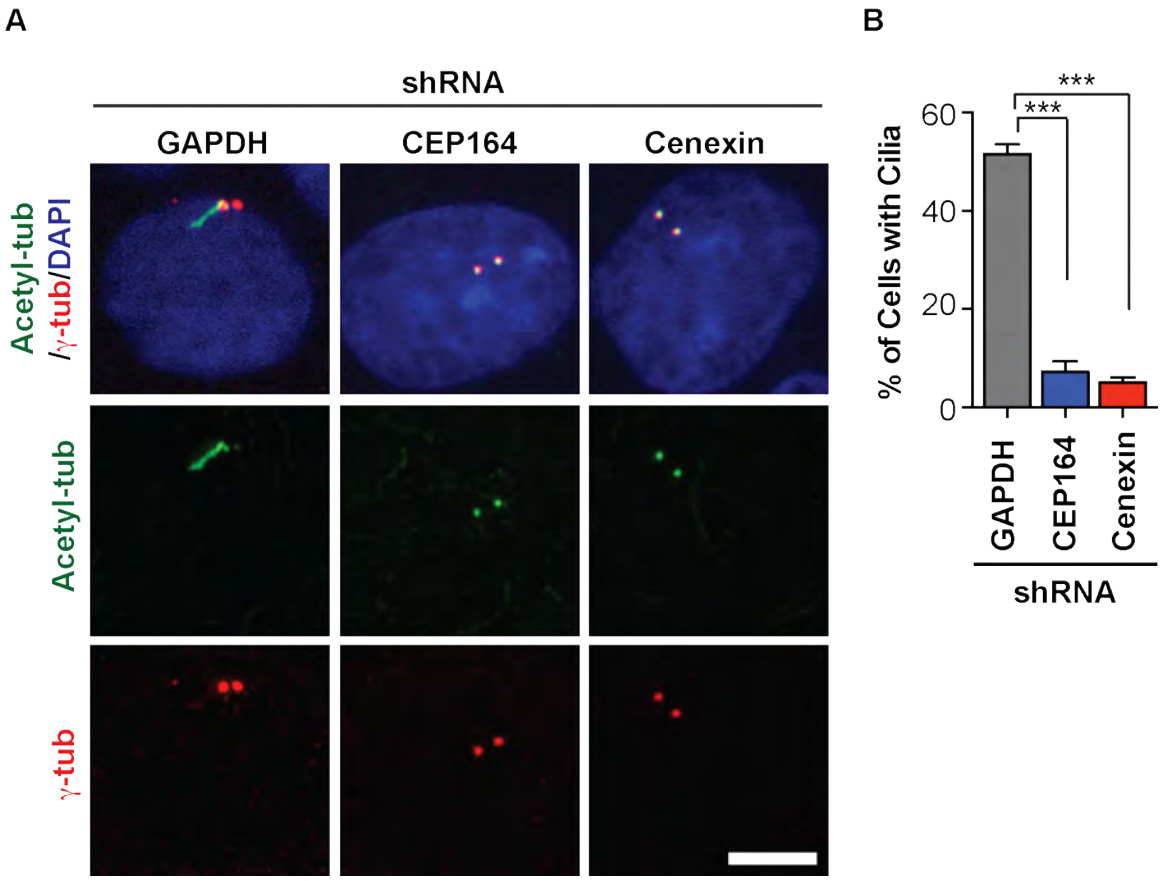

Figure 2.3 Depletion of CEP164 or cenexin caused ciliogenesis defects.
MDCK cells treated with shRNAs targeting CEP164 or cenexin were defective in ciliogenesis when compared to control (GAPDH shRNA).
(A) Cells were seeded at confluence on 0.4 μm transmembrane and cultured in serum-free conditions for 5 days. Cells were fixed with cold methanol and stained for cilia (acetylated tubulin, green), centrosomes (γ-tubulin, red), and nuclei (DAPI, blue). Scale bar, 5 μm.
(B) The percentage of cells having cilia was calculated for n=3 experiments. Data are represented as mean ± SD. >50 cells were counted in each group. ***, *p*-value <0.001.

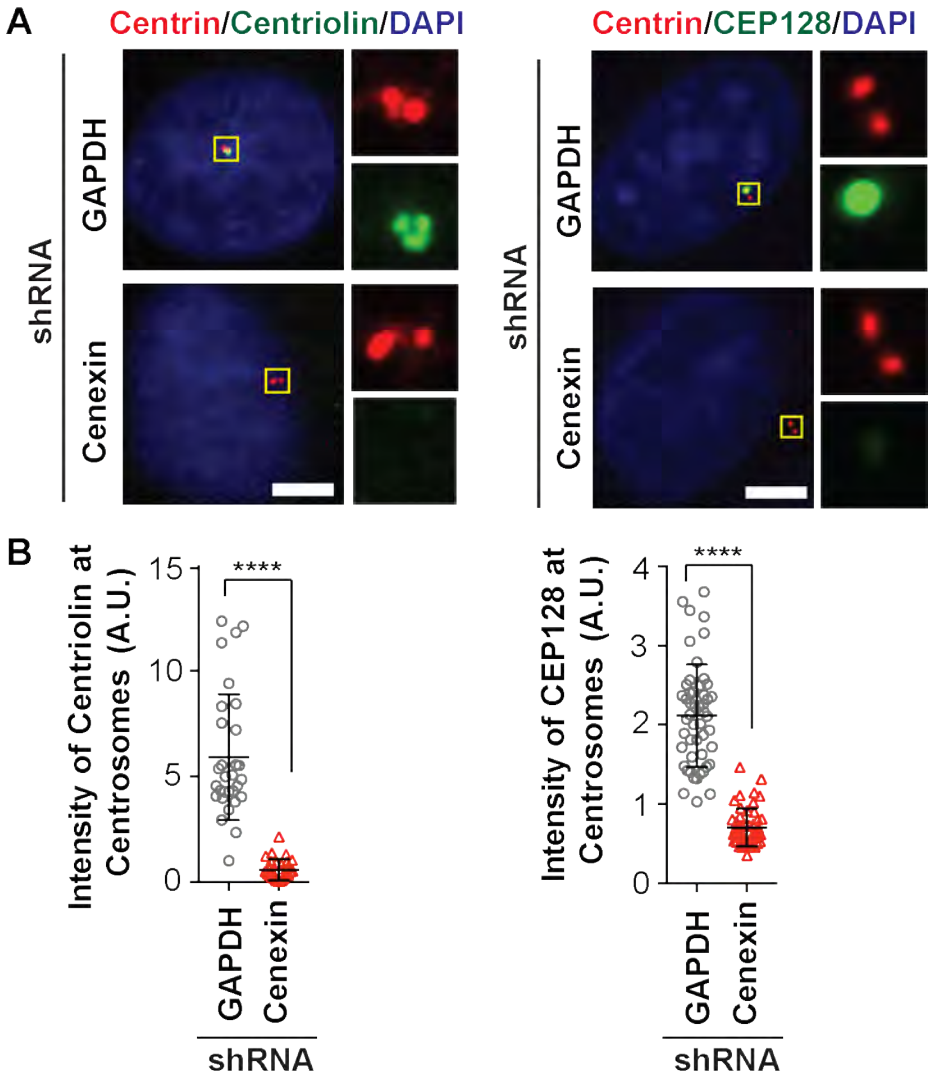

Figure 2.4 Subdistal appendage proteins are lost after cenexin depletion.
(A) The subdistal appendage proteins, centriolin (left) and CEP128 (right) at interphase centrosomes were displaced from the mother centrioles in cenexin-depleted U2OS cells. Centrosomes were stained for centrin (red), centriolin or CEP128 (green), and nuclei (DAPI, blue). Insets depict 4.5x magnification of the centrosome region. Scale bar, 5 μm. (B) The integrated intensity of centriolin (left) or CEP128 (right) at centrosomes measured in U2OS cells depleted of GAPDH and cenexin. Data are represented as mean ± SD of >30 centrosomes in each group. ****, *p*-value <0.0001.

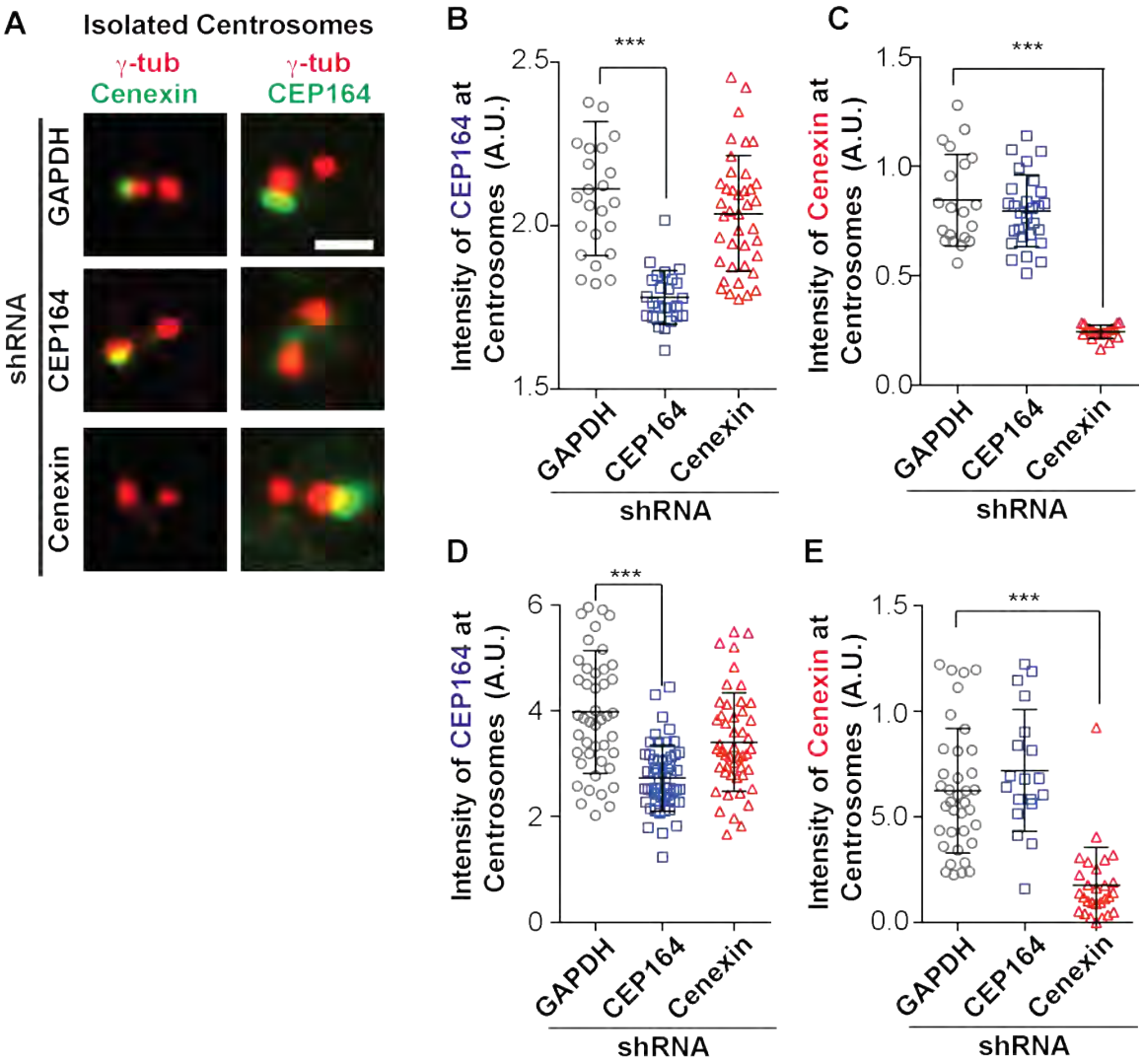

Figure 2.5 Loss of subdistal appendages does not perturb distal appendages and vice versa.

(A) Isolated interphase centrosomes from U2OS cells that express GAPDH-, CEP164-, or cenexin-shRNAs. Mother centrioles were decorated with antibodies against the distal appendage protein, CEP164 (right column, green), the subdistal appendage protein, cenexin (left column, green), and centrioles (γ-tubulin, red). Scale bar, 1 μm.

(B, C) and (D, E) The integrated intensity of CEP164 (B, D) or cenexin (C, E) at centrosomes in U2OS cells (B, C) and in MDCK cells (D, E) depleted of GAPDH, CEP164 and cenexin. Data are represented as mean ± SD of >20 centrosomes in each group. *** depicts a p-value <0.001.

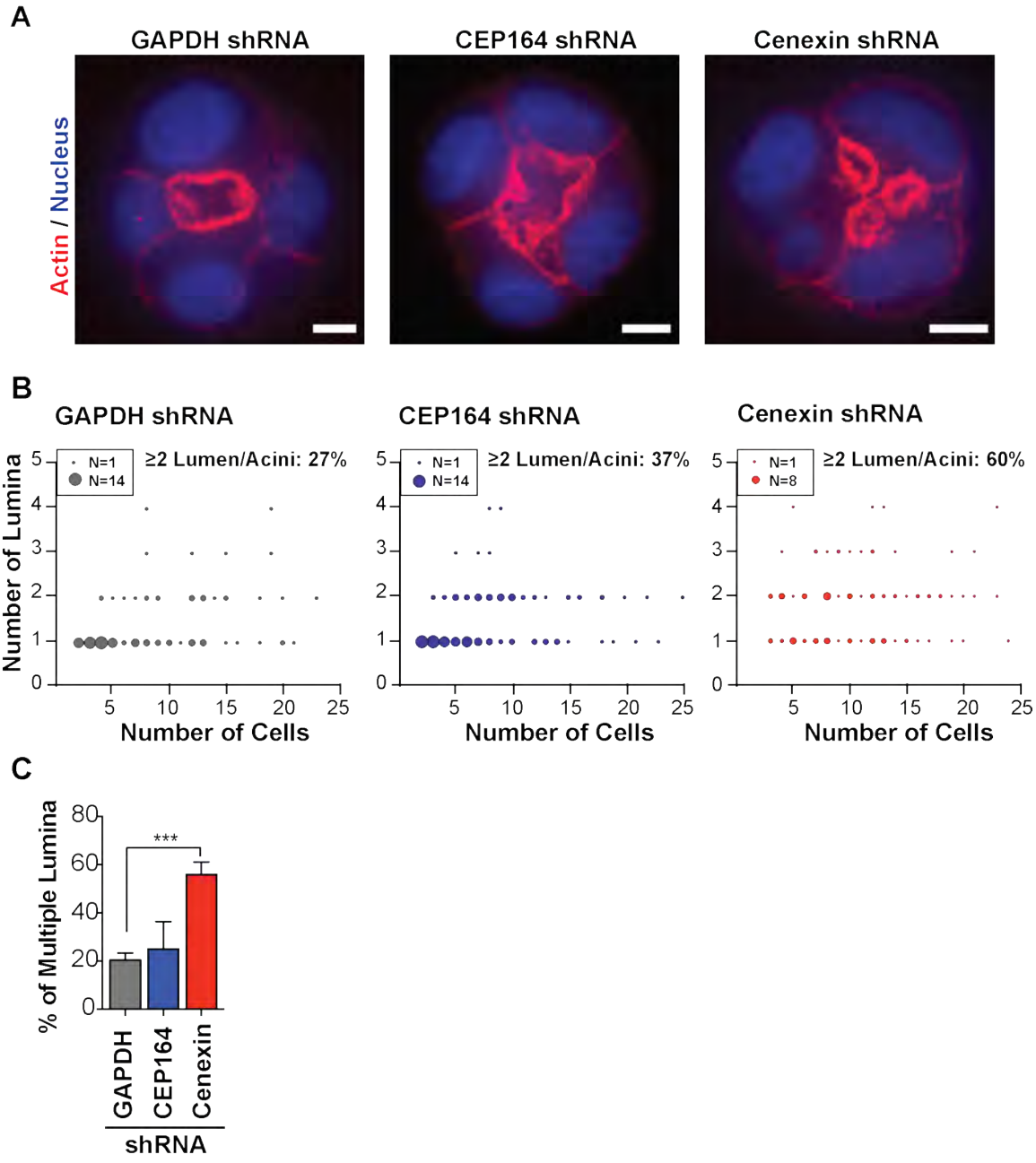
A
GAPDH shRNA
CEP164 shRNA
Cenexin shRNA
Actin / Nucleus
B
GAPDH shRNA
CEP164 shRNA
Cenexin shRNA
N=1
N=14
≥2 Lumen/Acini: 27%
≥2 Lumen/Acini: 37%
N=8
≥2 Lumen/Acini: 60%
Number of Lumina
Number of Cells
C
% of Multiple Lumina
***
GAPDH
CEP164
Cenexin
shRNA

Figure 2.6 Cenexin depletion leads to multiple lumina formation during early cyst development.

(A) 3D-cultured MDCK acini were fixed and stained for actin (phalloidin, red) and nuclei (DAPI, blue). A single confocal z-section at the center of the acinus is displayed. Scale bar, 5 μm.

(B) Scatter plot illustrating the number of lumina in different acini. The number of acini with a given number of lumen in the population correlates to the size of each point (refer to legend for each graph). Each graph represents >100 acini scored over 3 independent experiments.

(C) The percentage of acini with >1 lumen in MDCK 3-D cultured cells depleted of GAPDH, CEP164, or cenexin. Data are represented as mean ± SD from 3 independent experiments. >30 acini were counted in each group per experiment. ***, *p*-value <0.001.

Cenexin is required for centrosome positioning in interphase.

During interphase, centrosome positioning near the cell centroid is crucial for directional cell migration. Pathways involving cell polarity proteins and regulation of microtubule dynamics are emerging as common regulators of centrosome positioning in a variety of contexts (Elric and Etienne-Manneville, 2014; Luxton and Gundersen, 2011). Thus, we first investigated whether cenexin depletion disrupts apical-basolateral polarity in epithelial cells. Neither cenexin depletion nor CEP164 depletion disrupted the adherens junction protein, E-cadherin, or the apical membrane polarity proteins, PAR3 and PKCζ localization (Figure 2.7) (Rodriguez-Boulan and Macara, 2014), suggesting that cenexin and CEP164 are not involved in polarity establishment.

We further tested if cenexin was involved in centrosome positioning by exploiting micropatterned surfaces to generate cells with nearly identical shapes and sizes (refer to Figure 2.8A, left) (Théry et al., 2006). Centrosomes in nearly all control cells (GAPDH-depleted) localized within a 7 μm radius (dashed circle, Figure 2.8B) of the cell centroid. Strikingly, in cenexin-depleted cells, there was a six-fold increase in the percentage of centrosomes outside the centroid (30% compared to 5% in control cells and 3% in cells depleted of CEP164; Figure 2.8B and 2.8C). Moreover, cenexin depletion did not induce overt defects in microtubule nucleation at the centrosome (Figure 2.9) (Ibi et al., 2011), but did cause defects in microtubule focusing at this site (Figure 2.8A) (Ibi et al., 2011). This suggested that defects in microtubule focusing disrupt centrosome positioning. To examine the contribution of microtubule organization and stability in centrosome positioning, we took two approaches: 1) Depletion of two well-established centrosome-localized

modulators of microtubule nucleation, anchoring, and/or organization, PCM1 (Dammermann and Merdes, 2002) and pericentrin (PCNT) (Dictenberg et al., 1998; Doxsey et al., 1994; Zimmerman et al., 2004) and by 2) treatment with the microtubule-destabilizing drug, nocodazole.

PCM1- or PCNT-depletion caused only a subtle effect on centrosome centering (4%-10% not centered) (Figure 2.10A and 2.10D) compared to cenexin depletion (30%). Importantly, cenexin loss did not affect the presence of PCM1 or PCNT at the centrosome (Figure 2.10G and 2.10H) suggesting that cenexin, but not PCM1 or PCNT, has a significant role in centrosome positioning. PCM1 is involved in microtubule anchoring (Dammermann and Merdes, 2002), but it is possible that cenexin anchors a separate subset of microtubules that predominate during centrosome positioning highlighting cenexin in centrosome centering and microtubule focusing.

In a second experiment, we directly tested if microtubule dynamics were important for centrosome positioning by treating cells with nocodazole (4 nM, 10 nM, and 20 μM) to destabilize microtubules (Figure 2.11) (Vasquez et al., 1997). Cells treated with low concentrations of nocodazole (4-10 nM) exhibited significant centrosome displacement from the cell's centroid region similar to that seen in cenexin-depleted cells. Since cenexin depletion seemed to disrupt microtubules at the centrosome (Figure 2.8A), we attempted to rescue centrosome centering by stabilizing these microtubules with the microtubule-stabilizing drug, taxol (Yvon et al., 1999). Taxol treatment robustly reversed the effects of

cenexin depletion allowing cells to re-center their centrosomes (Figure 2.12) suggesting that stably focused microtubules at the centrosome are required for centrosome positioning.

We confirmed the role of cenexin in centrosome positioning using a physiologically-relevant wound-healing assay. The percentage of centrosomes that reorient to a position between the nucleus and the leading edge of the cell during migration was calculated. Two hours after inducing cell migration, 50% of control cells (GAPDH-depleted) reoriented their centrosome toward the leading edge, while fewer CEP164- and cenexin-depleted cells reoriented their centrosomes (43% for CEP164 depletion; 42% for cenexin depletion). Six hours after application of a scratch wound, ~60% of control (GAPDH-depleted) and CEP164-depleted cells reoriented their centrosomes (Figure 2.13A and 2.13B). However, centrosome reorientation was observed in only 40% of cenexin-depleted cells (Figure 2.13B), and could be rescued with an shRNA-resistant form of cenexin (Figure 2.13C). We conclude that cenexin is essential for centrosome reorientation during migration, while CEP164 may be dispensable in this process.

Cenexin is critical for centrosome positioning in interphase via modulation of microtubule stability.

During migration, wound-edge migrating cells contain more centrosome-localized stable/acetylated microtubules (Palazzo et al., 2003). After application of a scratch wound in control cells (6 hours), prominent acetylated microtubule arrays focused at the centrosome were noted (Figure 2.14A, GAPDH-depleted cells). In contrast, cenexin-depleted cells showed a significant reduction of acetylated tubulin at the centrosome

concomitant with disorganized microtubules (Figure 2.14A), reminiscent of cenexin-depleted cells grown on micropatterns (Figure 2.8A). Taxol treatment of cenexin-depleted cells rescued microtubule organization (stabilized microtubules) at the centrosome, and centrosome reorientation. These findings (Figure 2.14), together with those on centrosome centering (Figure 2.8 and 2.12), suggest that the subdistal appendage protein, cenexin, is critical for adjusting the position of the centrosome during migration via modulation of microtubule stability.

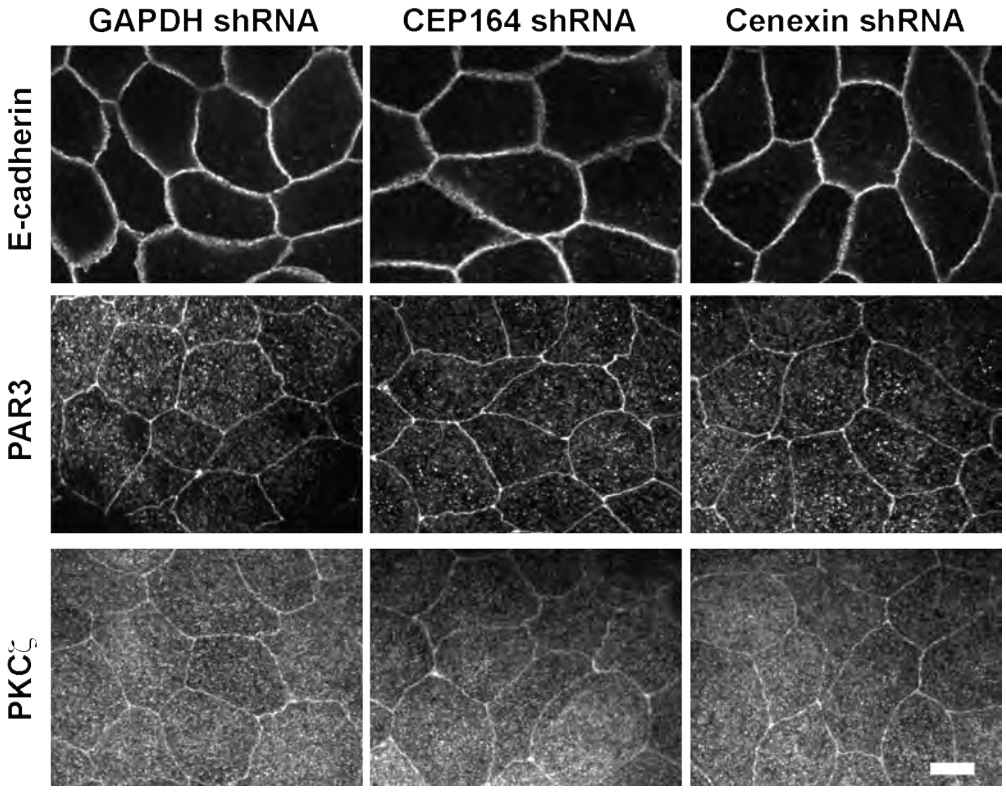

Figure 2.7 Depletion of CEP164 or cenexin does not affect the overall polarity of epithelial cells.

Depletion of CEP164 or cenexin did not affect localization of E-cadherin (top row), PAR3 (middle row), and PKCζ (bottom row) in polarized MDCK cultures. Cells were grown on transwell membranes (0.4 μm pore size) for 5 days under serum-free conditions. Scale bar, 10 μm.

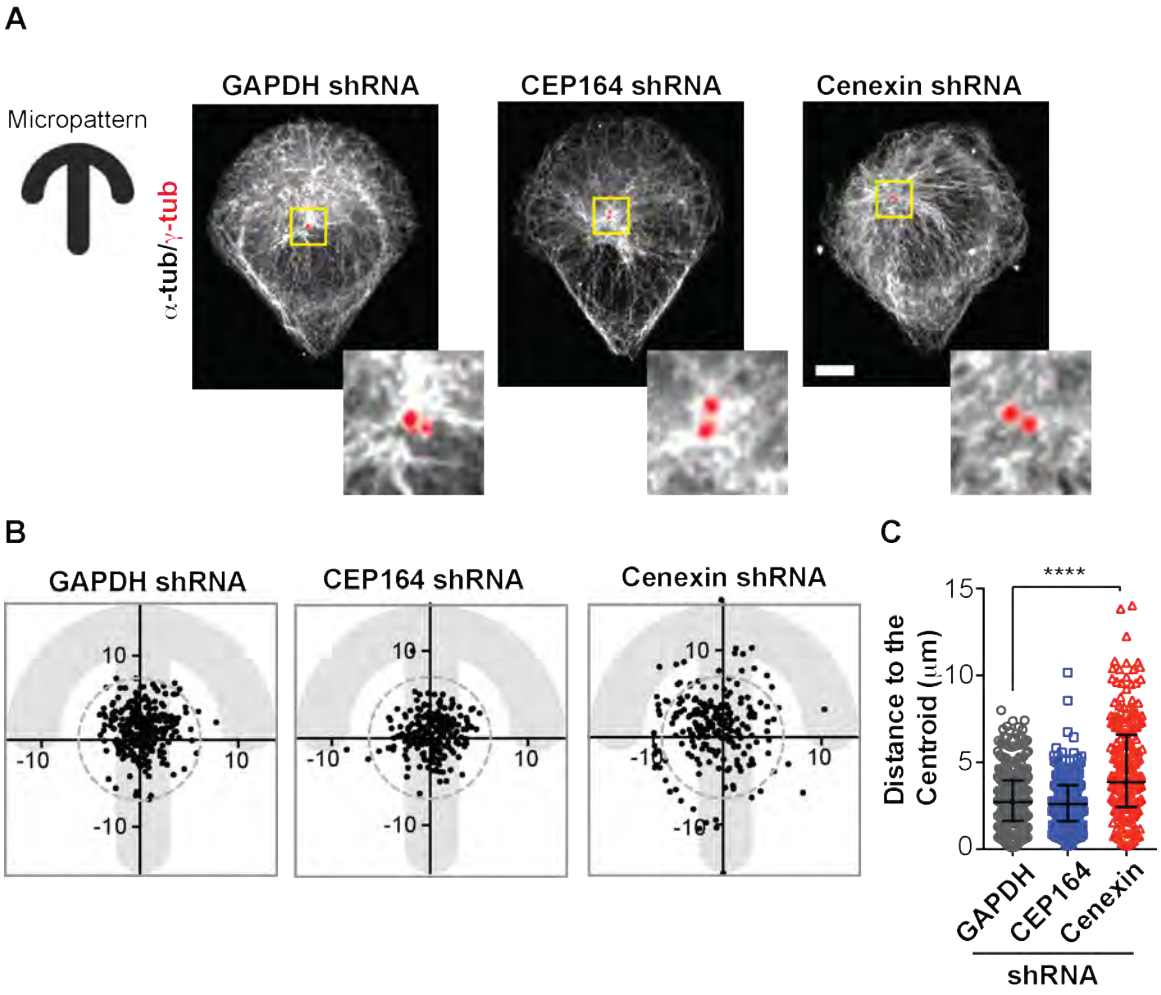
A
Micropattern
GAPDH shRNA
CEP164 shRNA
Cenexin shRNA
α-tub/γ-tub
B
GAPDH shRNA
CEP164 shRNA
Cenexin shRNA
10
-10
C
****
Distance to the Centroid (μm)
15
10
5
0
GAPDH
CEP164
Cenexin
shRNA

Figure 2.8 Cenexin is required for interphase centrosome centering.

(A) Left, Fibronectin-coated-crossbow micropattern on glass coverslips was used to mimic a migrating cell with a uniform cell shape and size. Right, U2OS cells were seeded onto micropatterns and stained for microtubules (α–tubulin, white) and centrosomes (γ-tubulin, red). Scale bar, 10 μm. Insets at the right of main images depict a 4x-magnified projection of microtubule anchoring at the centrosome. Cenexin-depleted cells show fewer microtubules focused at centrosomes.

(B) Interphase centrosome positions in cells grown on crossbow micropatterns. 270 centrosomes were plotted for the control cells, and 200 centrosomes were plotted for CEP164- depleted or cenexin- depleted cells. The centroid position in the pattern was determined and a circle with the radius of 7 μm was drawn. All points that fall outside of the circle were considered non-centered. Data were collected from >3 independent experiments.

(C) Distances between centrosomes and the cell centroid shown in (B) for GAPDH-, CEP164-, and cenexin-depleted cells. Data are represented as median ± interquartile range. ****, *p*-value<0.0001.

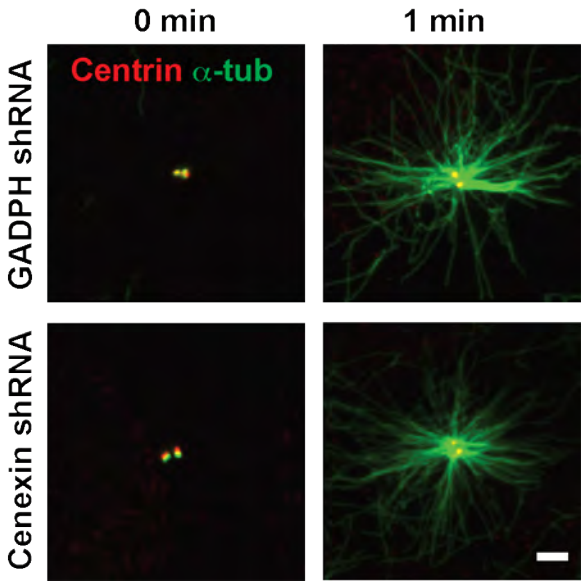

Figure 2.9 Cenexin-depleted centrosomes retain the ability to nucleate microtubules.

U2OS cells were treated with 20 μM of nocodazole for 2 hours to depolymerize all the microtubules. Cells were then washed with medium and incubated at 37°C for microtubule regrowth. Cells were fixed in cold methanol at the indicated time for microtubule regrowth and prepared for immunofluorescence staining. Centrosomes (centrin, red), and microtubules (green). Scale bar, 1 μm.

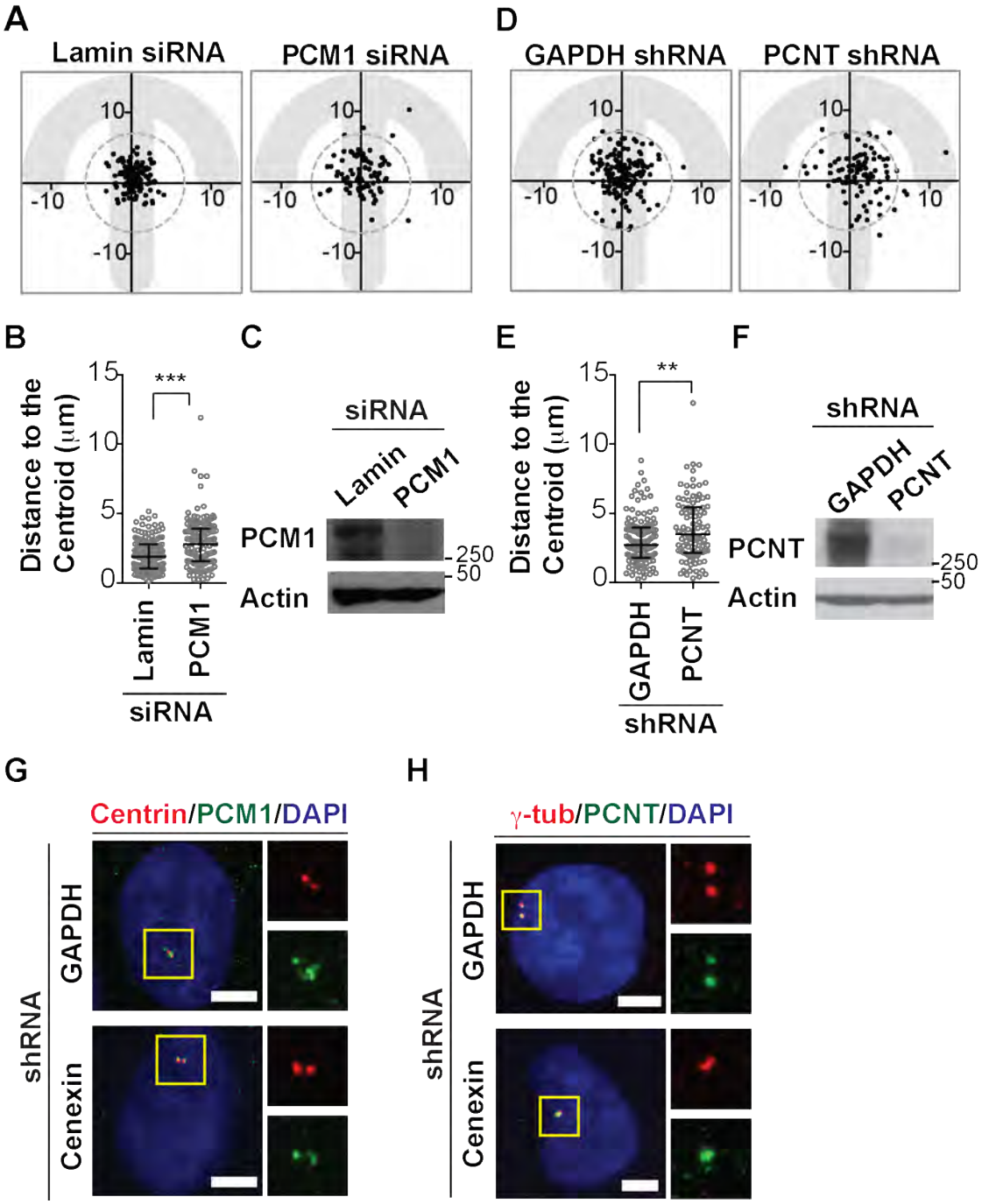
A
Lamin siRNA
PCM1 siRNA
D
GAPDH shRNA
PCNT shRNA
10
-10
B
Distance to the Centroid (μm)
15
10
5
0
***
Lamin
PCM1
siRNA
C
siRNA
Lamin
PCM1
PCM1
Actin
250
50
E
**
GAPDH
PCNT
shRNA
F
shRNA
GAPDH
PCNT
PCNT
Actin
G
Centrin/PCM1/DAPI
shRNA
GAPDH
Cenexin
H
γ-tub/PCNT/DAPI

Figure 2.10 Pericentriolar proteins, PCM1 and pericentrin, have a subtle effect on centrosome centering.

(A) Interphase centrosome positions for >125 centrosomes are plotted for lamin-depleted (control) and PCM1-depleted U2OS cells using a previously published siRNA (Dammermann and Merdes, 2002).

(B) Distances between centrosomes and the cell centroid (shown in Figure 2.10A) are shown for lamin- and PCM1-depleted cells. Data are represented as median ± interquartile range. ***, *p*-value<0.001.

(C) Immunoblot analysis of U2OS whole cell lysates after cells were treated with control or PCM1 siRNA. Staining against PCM1 and actin (loading control) is shown.

(D) Interphase centrosome positions were measured from cells grown on crossbow micropattern slides. 164 centrosomes were plotted for the control cells (GAPDH-depleted), and 99 centrosomes for PCNT-depleted U2OS cells.

(E) Distances between the scored centrosomes and the cell centroid (shown in Figure 2.10D) for GAPDH- and PCNT-depleted cells were measured. Data are represented as median ± interquartile range. **, *p*-value<0.01.

(F) Immunoblot analysis of U2OS whole cell lysate treated with PCNT or control (GAPDH) shRNA. Staining with antibodies against PCNT and actin.

(G-H) The presence of PCM1 (G) or PCNT (H) at interphase centrosomes was not decreased in cenexin-depleted U2OS cells. Cells were stained for centrosomes (centrin or γ-tubulin, red), and PCM1 or PCNT (green). Insets depict 2x magnification of the centrosome region. Scale bar, 5 μm.

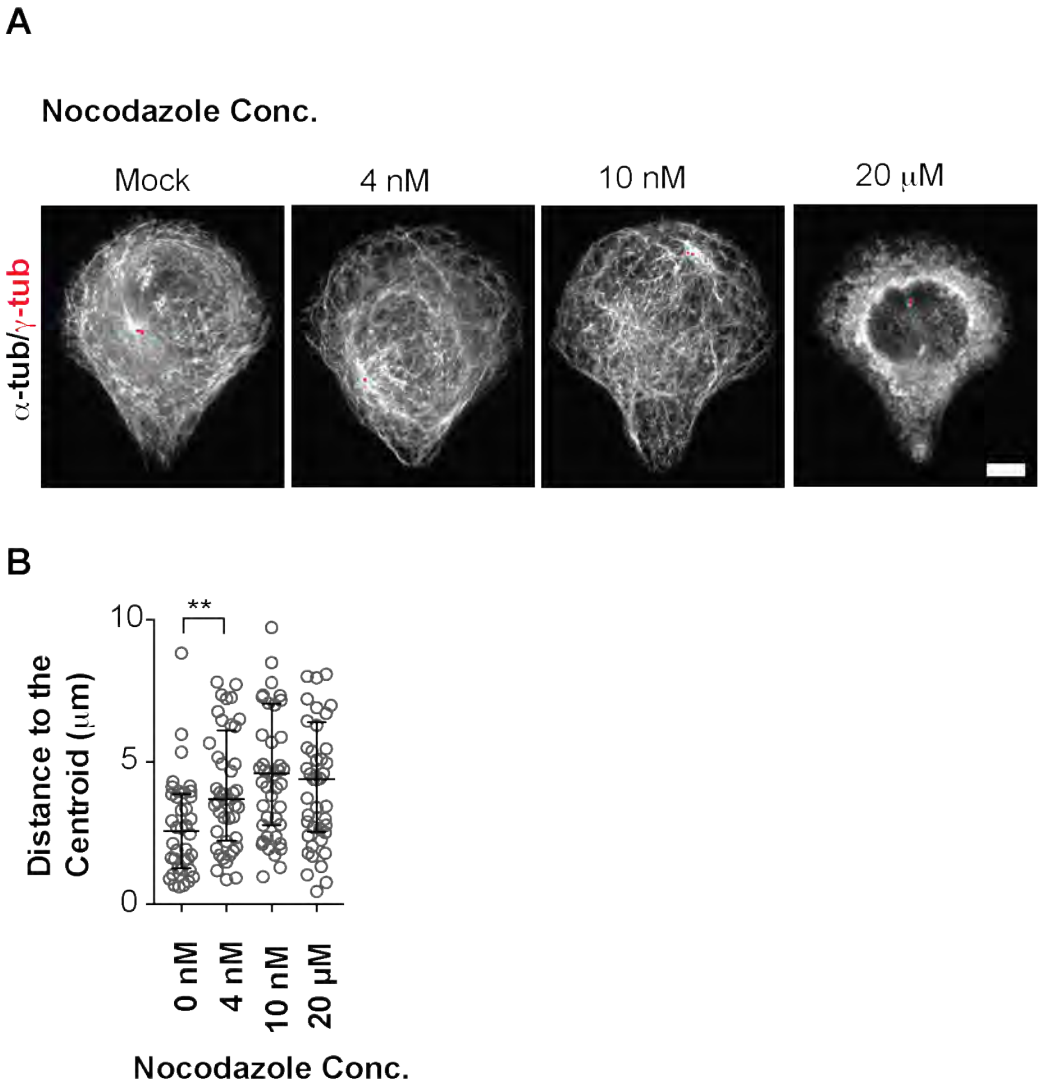

Figure 2.11 Microtubule dynamics are involved in centrosome positioning.
(A) U2OS cells were grown on crossbow micropatterned slides and treated with nocodazole (mock, 4 nM, 10 nM, and 20 μM), and stained for microtubules (α-tubulin, white) and centrosomes (γ-tubulin, red). Scale bar, 10 μm.
(B) Distances between centrosomes and the cell centroid with various nocodazole treatments. Data are represented as median ± interquartile range of >50 cells/treatment. Representative of n=2 experiments. **, *p*-value <0.01.

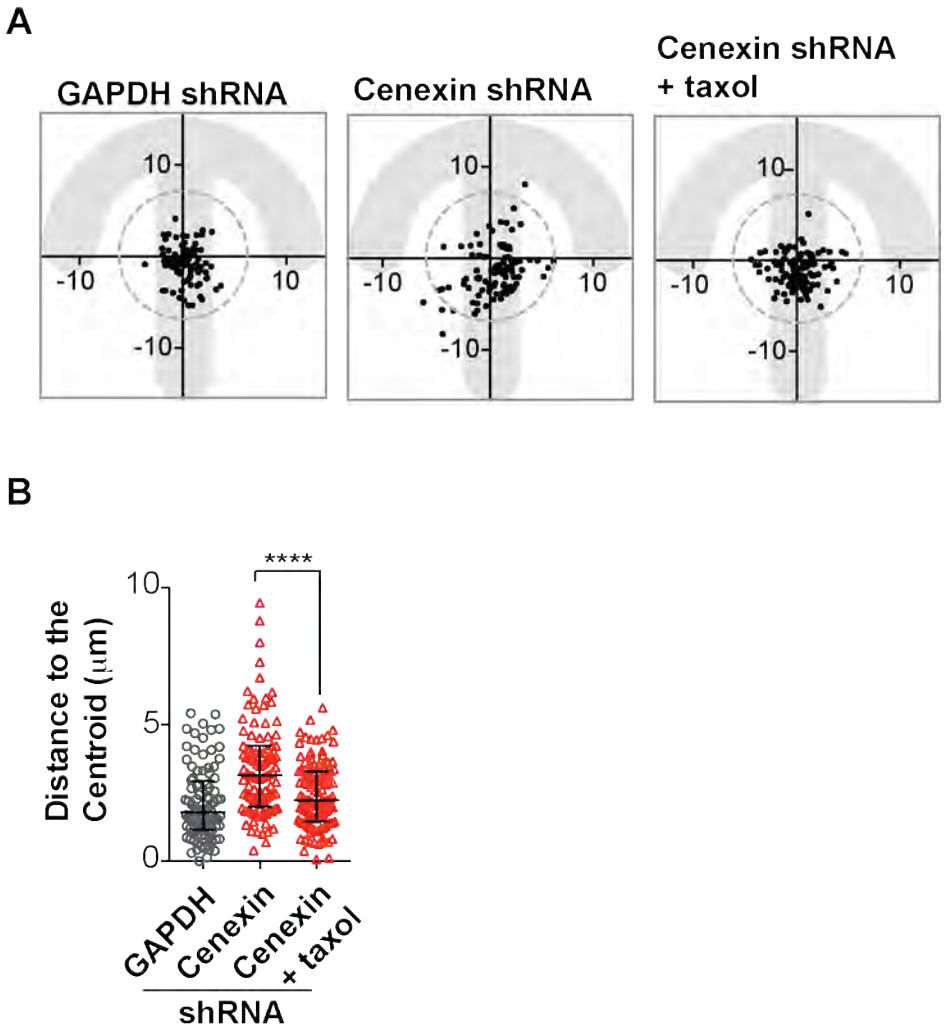

Figure 2.12 Stabilizing microtubules with taxol treatment rescues the centrosome centering defect in cenexin-depleted cells.

(A) Interphase centrosome positions in cells grown on crossbow micropatterns were treated with or without taxol as labeled; 100 centrosomes were plotted in each group.

(B) Distances between centrosomes and the cell centroid shown in (A). Data are represented as median ± interquartile range. ****, *p*-value<0.0001.

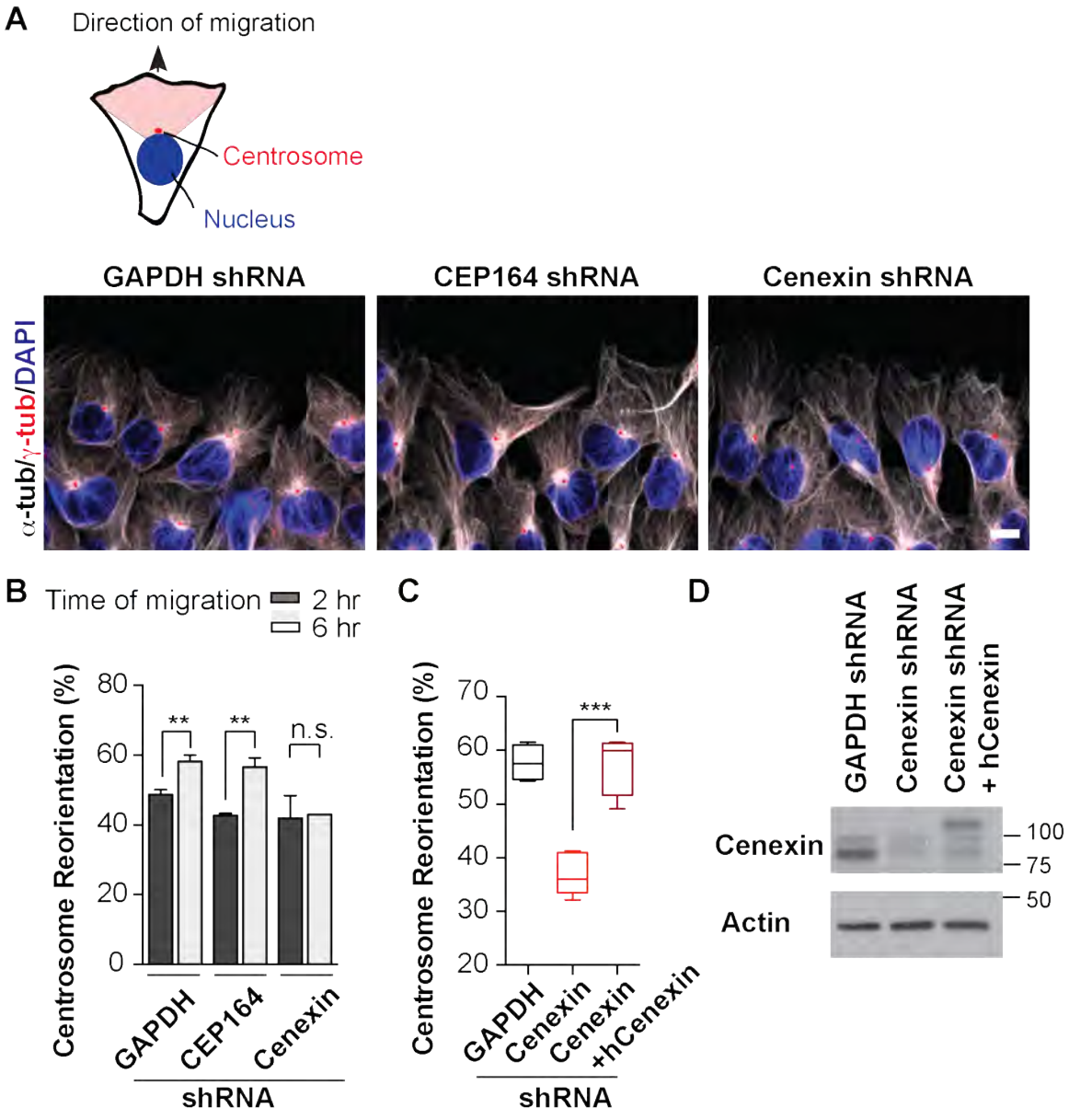
A
Direction of migration
Centrosome
Nucleus
GAPDH shRNA
CEP164 shRNA
Cenexin shRNA
α-tub/γ-tub/DAPI
B
Time of migration
2 hr
6 hr
Centrosome Reorientation (%)
80
60
40
20
0
**
**
n.s.
GAPDH
CEP164
Cenexin
shRNA
C
Centrosome Reorientation (%)
70
60
50
40
30
20
***
GAPDH
Cenexin
Cenexin +hCenexin
shRNA
D
GAPDH shRNA
Cenexin shRNA
Cenexin shRNA + hCenexin
Cenexin
Actin
100
75
50

Figure 2.13 Cenexin is required for centrosome reorientation during cell migration.

(A) Top row, a model depicting centrosome (red) localization during migration. Upon inducing cell migration, the centrosome reorients into the light red quadrant in front of the nucleus (blue) towards the direction of migration. Bottom row, U2OS cells depleted of GAPDH (control), CEP164, or cenexin were fixed and stained for centrosomes (γ-tubulin, red), nuclei (DAPI, blue), and microtubules (α-tubulin, white) 6-hours after scratch wound application. Scale bar, 10 μm.

(B) The percentage of centrosomes that orient towards the front quadrant (modeled in Figure 2.13A top row, light red section) at 2 hours (dark grey) and 6 hours (light grey) after scratch wound application. Cells were depleted of GAPDH, CEP164, or cenexin. Data are represented as mean ± SEM for 3 independent experiments, and >200 cells were counted in each group/experiment. **, p-value<0.01. n.s. = not significant.

(C) U2OS cells depleted of GAPDH or cenexin, and subsequently rescued with an shRNA-resistant human cenexin were scored for centrosome reorientation towards the leading edge 6-hours after scratch wound application. Data are represented as a box-and-whisker plot with max and min of >300 cells over 3 regions in each group. Representative of n=2 experiments. ***, p-value<0.001.

(D) Immunoblot analysis of U2OS whole cell lysates after cells were transfected with control or cenexin expression constructs. Staining against cenexin and actin (loading control) is shown.

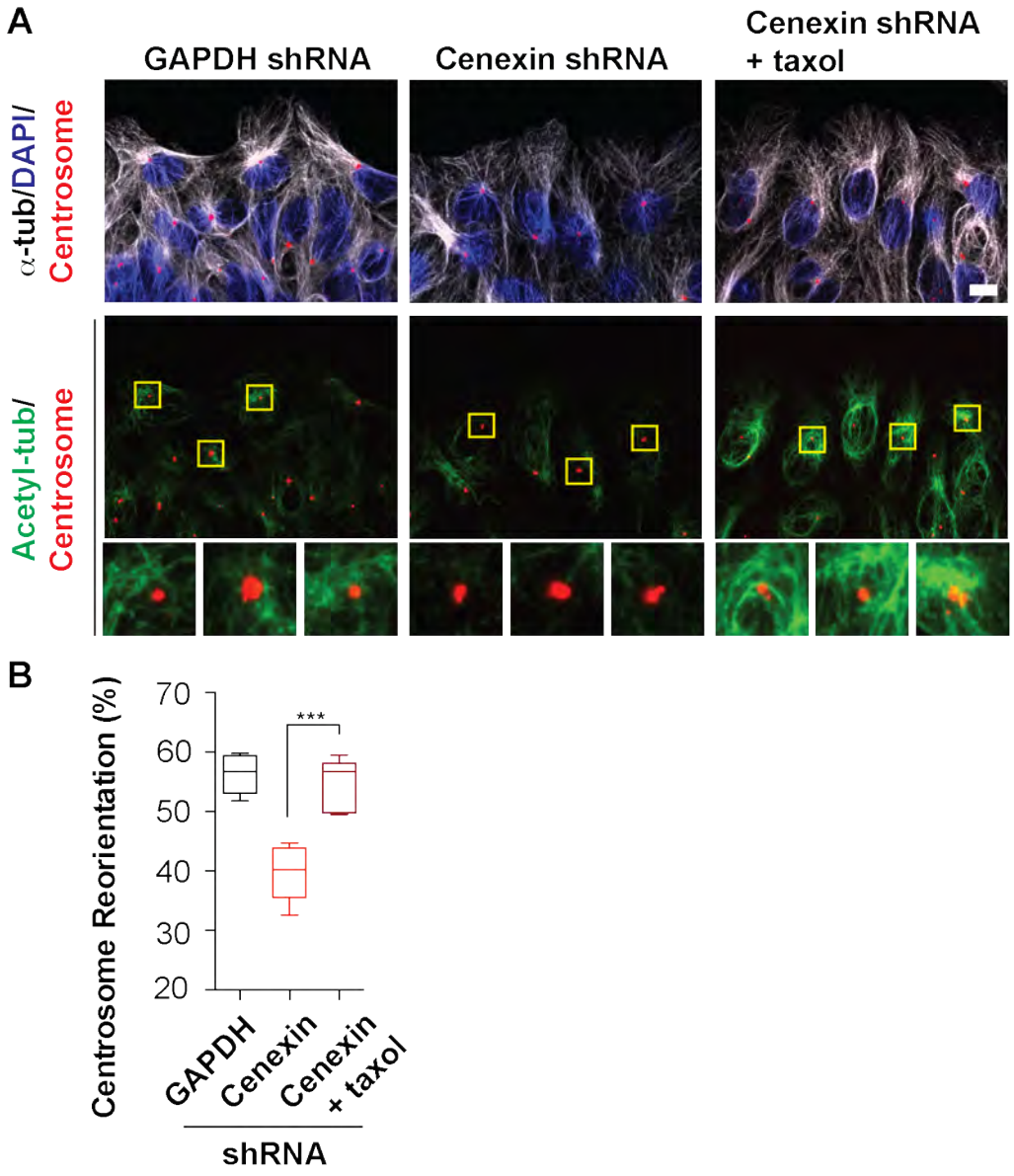
A
GAPDH shRNA
Cenexin shRNA
Cenexin shRNA
+ taxol
α-tub/DAPI/
Centrosome
Acetyl-tub/
Centrosome
B
Centrosome Reorientation (%)
70
60
50
40
30
20
***
GAPDH
Cenexin
Cenexin
+ taxol
shRNA

Figure 2.14 Loss of acetylated microtubules at the centrosomes with cenexin-depletion during cell migration.

(A) U2OS cells (GAPDH-depleted, cenexin-depleted, and cenexin-depleted cells treated with taxol) were fixed 6 hours after applying a scratch wound. Top row, cells were stained with centrosomes (pericentrin, red), microtubules (α−tubulin, white), and nuclei (DAPI, blue). Bottom row, cells were stained for acetylated microtubules (green), and centrosomes (pericentrin, red). Insets, below main images, depict a 4x-magnified projection of acetylated microtubules at the centrosome. Scale bar, 10 μm.

(B) The percentage of centrosomes that orient towards the front quadrant (A) at 6 hours after applying a scratch wound. Data are represented as a box-and-whisker plot with max and min of >300 cells over >3 regions in each group. Representative of n=2 experiments. ***, *p*-value<0.001.

Cenexin regulates mitotic spindle pole positioning and thus, spindle orientation.

During mitosis, spindle pole integrity and function are crucial for spindle orientation. In fact, loss of function of spindle pole proteins can affect astral microtubule dynamics and spindle orientation (Barros et al., 2005; Chen et al., 2014; Delaval et al., 2011; Hehnly and Doxsey, 2014; Hehnly et al., 2015; Thaiparambil et al., 2012). Moreover, proper control of division orientation is required for the symmetric expansion of a central lumen in a growing acinus and for the development of a variety of organs (modeled in Figure 2.1, (Blasky et al., 2015; Overeem et al., 2015)). For these reasons, we tested if appendages were present in spindle poles/mitotic centrosomes and if cenexin and CEP164 localized to these structures, as they did in interphase cells. Mitotic cells processed for transmission electron microscopy (TEM) showed that one of the two centrioles in mitotic centrosomes contained both subdistal and distal appendages (Figure 2.15A). We next determined that cenexin and CEP164 displayed conventional appendage-like localization at the subdistal and distal appendages of mitotic centrioles suggesting that both CEP164 and cenexin maintained their appendage localization during mitosis (Figure 2.15B). In support of previous studies (Lange and Gull, 1995), cenexin accumulated primarily at appendages of the older centriole (Figure 2.15C, top, and quantification of >30 cells in Figure 2.15D, left). Interestingly, the intensity difference of CEP164 between the two spindle poles was not as significant as cenexin (Figure 2.15C and 2.15D). These findings suggest that differential localization of cenexin to the poles might contribute to proper spindle orientation (Yamashita, 2009).

CEP164 or cenexin was depleted and tested for changes in spindle positioning during mitosis (Figure 2.16E). Only cenexin-depleted cells showed variability in the orientation of their spindle to the substratum (Figure 2.16A, 2.16B, and 2.16E). More specifically, 50% of cenexin-depleted cells demonstrated a spindle angle >5°, whereas most control spindles were parallel to the substratum (<5°, 75% for control). CEP164-depleted cells displayed a modest difference compared to control (<5°, 68% for CEP164; Figure 2.16B and 2.16E). Importantly, spindle orientation defects could be rescued by expressing an shRNA-resistant form of cenexin (Figure 2.16A-D and 2.16F-G). We observed similar defects in U2OS cells (Figure 2.16H) or when additional shRNAs were used (Figure 2.16I) further demonstrating that the subdistal appendage protein, cenexin, but not the distal appendage protein, CEP164, is essential for modulating spindle orientation.

We found that spindle misorientation in cenexin depleted cells was the likely cause of multi-lumina formation in acini (as in Figure 2.6A and 2.6B). In control acini (GAPDH depletion), the spindle was nearly parallel to the apical lumen in most cells (on average 18°, Figure 2.17A and 2.17B), suggesting that spindle alignment contribute to normal symmetric lumen expansion. However, in cenexin-depleted cells, a higher degree of spindle angle variability and an overall increase in spindle angle towards the apical lumen was observed (Figure 2.17A and 2.17B). Taken together, these results indicate that cenexin is required for control of spindle orientation and single lumen formation. Importantly, taxol treatment rescued spindle misorientation in cenexin-depleted cells, as there was a significant decrease in the spindle angle in relation to the lumen under these conditions

(Figure 2.17C and 2.17D), This suggests that cenexin regulates microtubule stability that influences centrosome positioning in both non-dividing and mitotic cells.

Cenexin depletion decreases astral microtubule number and length in mitotic cells.

To better understand the role of cenexin in spindle positioning we examined the overall morphology of the mitotic spindle in cenexin-depleted cells. Astral microtubule arrays in cells depleted of cenexin were disrupted when compared to control cells (GAPDH-depleted, Figure 2.18A). The plus-end microtubule binding protein EB1 was used to visualize astral microtubules and revealed a significant decrease in both astral microtubule number (30% of control, Figure 2.18B) and length (17% of control, Figure 2.18C) in cenexin depleted cells. Having observed defects in the astral microtubule plus ends (EB1 staining), we examined the minus ends at the poles by visualizing the minus-end binding protein, KIF2A (Ganem and Compton, 2004). Interestingly, we observed a significant defocusing of KIF2A at spindle poles in cenexin-depleted cells compared to controls (Figure 2.18D), while the presence of KIF2A at the spindle poles was unchanged (Figure 2.18E). This suggests that cenexin loss causes disorganization of microtubule minus-ends, which can lead to defects in anchoring, stability, and/or growth of astral microtubules. Cenexin depletion did not affect spindle pole localization of canonical spindle pole proteins involved in microtubule nucleation and spindle orientation, namely γ-tubulin, pericentrin, and the pericentrin binding protein, CEP215 (Figure 2.19A) (Chen et al., 2014; Zimmerman et al., 2004) nor did we observe any significant difference in cell cycling, mitotic progression, chromosome congression, kinetochore alignment or

kinetochore-fiber formation under these conditions (Figure 2.19B-2.19E, (Gasic et al., 2015)). Thus, we conclude that spindle microtubules, as well as microtubule-nucleating and -depolymerizing activity at the spindle pole are not grossly affected in cenexin-depleted cells, whereas cenexin is required for proper organization of astral microtubules.

Cenexin-depletion destabilizes astral microtubules and contributes to cortical NuMA mislocalization.

The interaction between astral microtubules and the cell cortex has been shown to direct spindle orientation. This process involves the NuMA/LGN/Gαi complex (NuMA complex), which is transiently organized at the cell cortex during metaphase, to assist in astral microtubule capture (Kotak and Gönczy, 2013). Since we observed spindle misorientation (Figure 2.16 and 2.17) and astral microtubule defects in cenexin-depleted cells (Figure 2.18), we hypothesized that cenexin depletion could disrupt the distribution of the NuMA complex at the cell cortex. Interestingly, we found that cenexin depletion in two separate cell lines (MDCK and U2OS) increased cortical NuMA localization when compared to control cells (Figure 2.20A-2.20D). These findings suggested that loss of astral microtubules caused by cenexin depletion, did not impede NuMA recruitment to the cell cortex, but instead, increased NuMA localization at this site.

NuMA may not require astral microtubules for delivery to the cell cortex (Kotak et al., 2014), but instead, it may require astral microtubules to dissociate from the cortex (Zheng et al., 2013). In fact, in our system, a second approach suggested the requirement for astral microtubules in cortical NuMA dissociation. Control cells treated with

nocodazole to selectively destabilize astral microtubules (Figure 2.21A) (Vasquez et al., 1997) showed a 5-fold increase in NuMA at the cell cortex compared to vehicle-treated cells (Figure 2.20E and 2.20F). This closely mimicked the phenotype of cenexin depletion (Figure 2.20A and 2.20B).

To further confirm that cenexin depletion affects the stability/growth of astral microtubules and therefore impedes NuMA dissociation from the cell cortex, taxol was used to stabilize astral microtubules (Figure 2.21C) (Yvon et al., 1999). A significant reduction in cortical NuMA was observed under these conditions compared to mock treated cenexin depleted cells (Figure 2.20G and 2.20HJ). The taxol treatment rescued the spindle misorientation phenotype in cenexin-depleted cells (1.6-fold, Figure 2.21D and 2.21E), while low-dose nocodazole treatment caused spindle misorientation in control cells (Figure 2.21B and 2.21E). Thus, we argue that astral microtubules loss observed in cenexin-depleted cells causes NuMA mislocalization at the cell cortex and spindle misorientation.

Cenexin-regulated subdistal appendages are required for ensuring appropriate lumenogenesis.

We present a model wherein the cenexin-regulated subdistal appendages are required for microtubule organization at the mother centriole (Figure 2.22) (Bornens, 2002; Kunimoto et al., 2012). In line with previous findings (Hehnly et al., 2012; Tanos et al., 2013), cenexin depletion causes subdistal appendage protein loss with no overt defects to distal appendages (Figure 2.5). We conclude that cenexin-regulated-subdistal appendages and not distal appendages are specifically required for centrosome positioning both in

interphase cells for proper directed migration (Figure 2.8 and 2.13), and during mitosis for appropriate placement and orientation of the mitotic spindle (Figure 2.16). In addition, our findings suggest that cenexin affects a specific pool of microtubules, namely astral microtubules, that influences spindle orientation and modulates localization of NuMA at the cell cortex (Figure 2.18 and 2.20). We reason that this regulation is required for apical-basal axis orientation and epithelial lumen positioning (Figure 2.16 and 2.17; modeled in Figure 2.22).

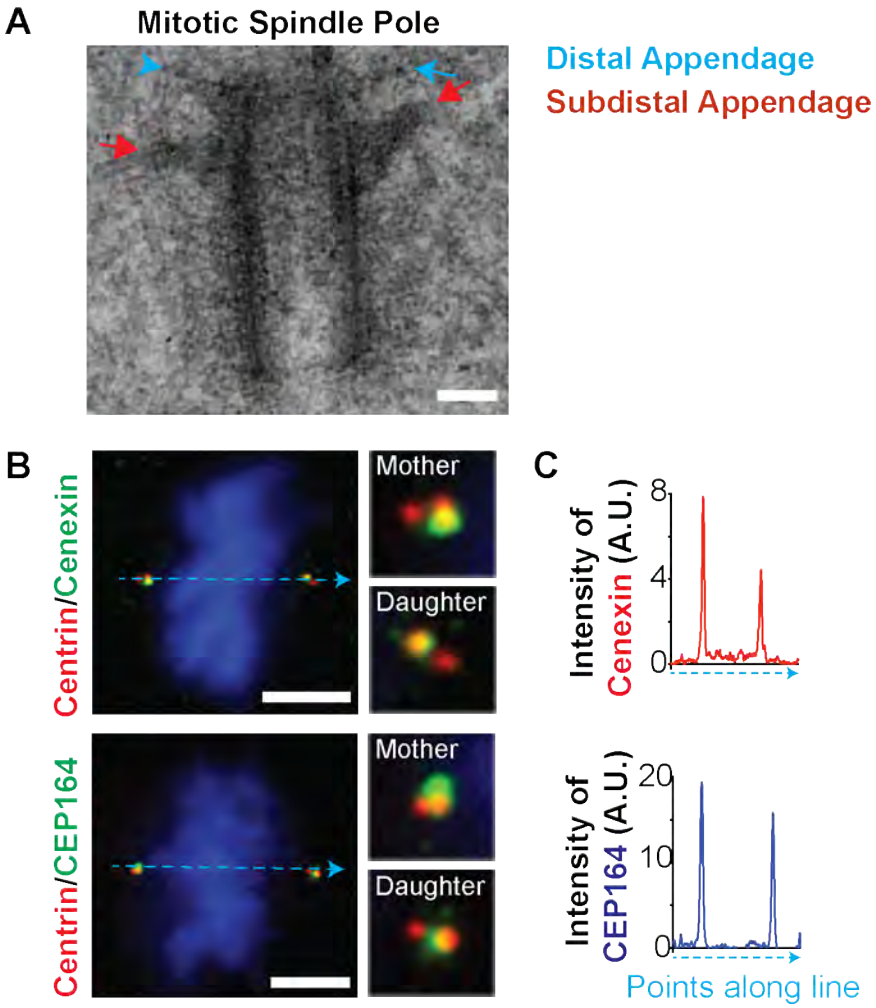
A
Mitotic Spindle Pole
Distal Appendage
Subdistal Appendage
B
Centrin/Cenexin
Mother
Daughter
Centrin/CEP164
Mother
Daughter
C
Intensity of Cenexin (A.U.)
8
4
0
Intensity of CEP164 (A.U.)
20
10
0
Points along line
D
Intensity of Cenexin at Spindle Poles (A.U.)
10
8
6
4
2
0
Mother
Daughter
Intensity of CEP164 at Spindle Poles (A.U.)
12
11
10
9
8
7
Mother
Daughter

Figure 2.15 Appendage proteins localize at mother centriole during mitosis.
(A) Mitotic cells were collected by mitotic shake-off and processed for transmission electron microscopy. Shown is a representative mother centriole from a mitotic spindle. Scale bar, 0.1 μm. The distal appendage is highlighted by a blue arrowhead, and the subdistal appendage is highlighted by a red arrow.
(B) Immunofluorescence staining of U2OS cells at metaphase; centrioles (centrin, red), CEP164 or cenexin (green). Dashed line (blue) depicts where line-scan measurements were obtained for (C). Scale bar, 5 μm. Insets depict 4x-magnification of mother and daughter spindle poles.
(C) Line scans through two spindle poles of images in (B). Upper image, demonstrates the presence of more cenexin on one pole (the mother/older spindle pole) than the other. Bottom image, depicts similar amounts of CEP164 intensity across two spindle poles.
(D) The integrated intensity of cenexin (left) or CEP164 (right) at the mother and daughter spindle poles were measured in >30 mitotic cells (U2OS). Data are represented as mean ± SD of >30 cells in each graph.

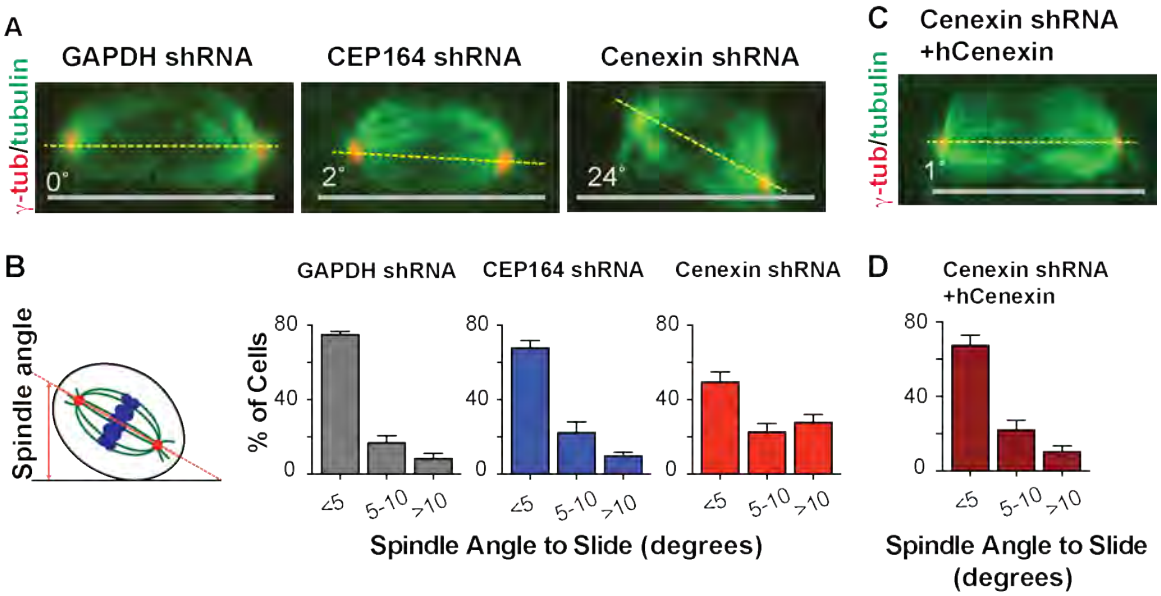
A
GAPDH shRNA
CEP164 shRNA
Cenexin shRNA
γ-tub/tubulin
0°
2°
24°
C
Cenexin shRNA
+hCenexin
γ-tub/tubulin
1°
B
Spindle angle
GAPDH shRNA
CEP164 shRNA
Cenexin shRNA
% of Cells
80
40
0
<5
5-10
>10
Spindle Angle to Slide (degrees)
D
Cenexin shRNA
+hCenexin
80
40
0
<5
5-10
>10
Spindle Angle to Slide
(degrees)

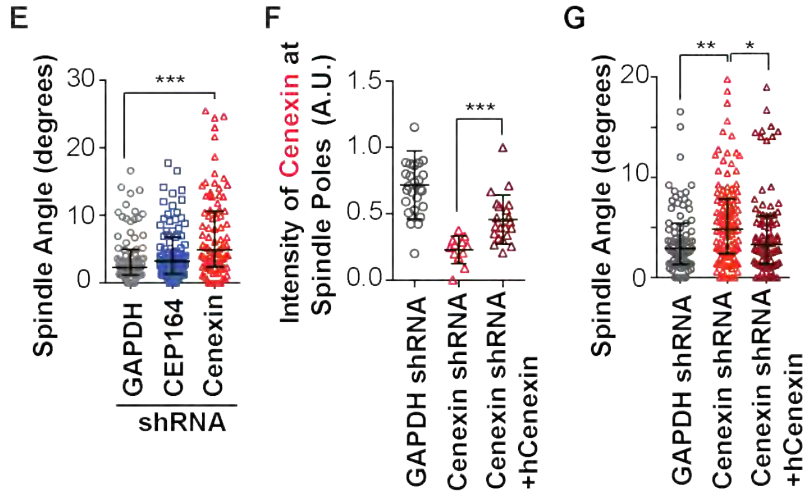
E
Spindle Angle (degrees)
30
20
10
0
***
GAPDH
CEP164
Cenexin
shRNA
F
Intensity of Cenexin at
Spindle Poles (A.U.)
1.5
1.0
0.5
0.0
***
GAPDH shRNA
Cenexin shRNA
Cenexin shRNA
+hCenexin
G
Spindle Angle (degrees)
20
10
0
**
*
GAPDH shRNA
Cenexin shRNA
Cenexin shRNA
+hCenexin

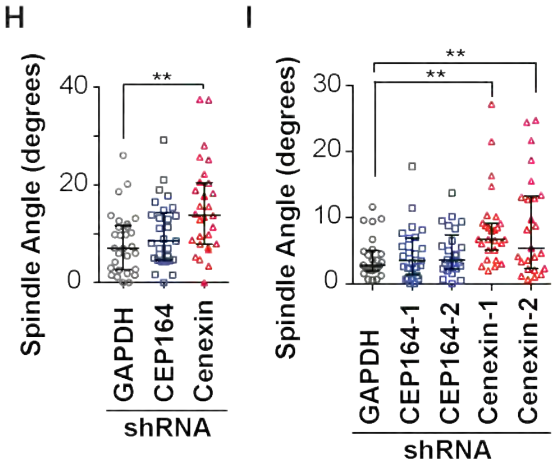
H
Spindle Angle (degrees)
40
20
0
**
GAPDH
CEP164
Cenexin
shRNA
I
Spindle Angle (degrees)
30
20
10
0
**
**
GAPDH
CEP164-1
CEP164-2
Cenexin-1
Cenexin-2
shRNA

Figure 2.16 Cenexin-depletion causes mitotic spindle tilting in polarized epithelial cell.

(A and C) Orthogonal view (x-z) of metaphase MDCK cells stained for microtubules (α-tubulin, green), and spindle poles (γ-tubulin, red) depleted of GAPDH, CEP164 or cenexin (A), and subsequently rescued with shRNA-resistant human cenexin (C). Grey line depicts the culture substrate, and yellow-dashed lines portray the orientation of spindles to substrates.

(B and D) Quantification showing a significant increase (>10°) in spindle angles from cells depleted of cenexin (3-fold) compared to control cells (GAPDH shRNA), while no significant change was seen in CEP164-depleted cells. Data are represented as mean ± SEM of 3 independent experiments with >25 cells measured in each treatment/ experiment.

(E) Collective raw spindle angles from (B) are shown. Data are represented as median ± interquartile range. ***, *p*-value <0.001.

(F) MDCK cells treated with GAPDH shRNA, cenexin shRNA, or cenexin shRNA plus an shRNA-resistant human cenexin construct were fixed and stained for cenexin. The integrated intensity of cenexin at mitotic spindle poles was measured for each treatment. Each dot represents the average intensity of two spindle poles in the cell, and mean ± SD is shown. >20 cells were measured for each group. ***, *p*-value <0.001.

(G) Collective raw spindle angles were measured and compared between MDCK cells depleted of cenexin and cells rescued with an shRNA resistant cenexin (D). Data are represented as median ± interquartile range. *, *p*-value<0.05. **, *p*-value<0.01.

(H) Demonstrates the raw spindle angles measured in U2OS cells depleted of GAPDH, CEP164, or cenexin. Data are represented as median ± interquartile range of 29 cells. **, *p*-value<0.01.

(I) Raw spindle angles were measured in MDCK cells treated with a GAPDH shRNA, and two different shRNAs towards either CEP164, or cenexin. CEP164-1 and cenexin-1 shRNAs were the same shRNAs used in (A-D). CEP164-2 and cenexin-2 shRNAs were additional shRNAs to confirm the protein depletion phenotype. Data are represented as median ± interquartile range. A representative of n=3 experiments is shown, n=25 cells/treatment. **, *p*-value<0.01.

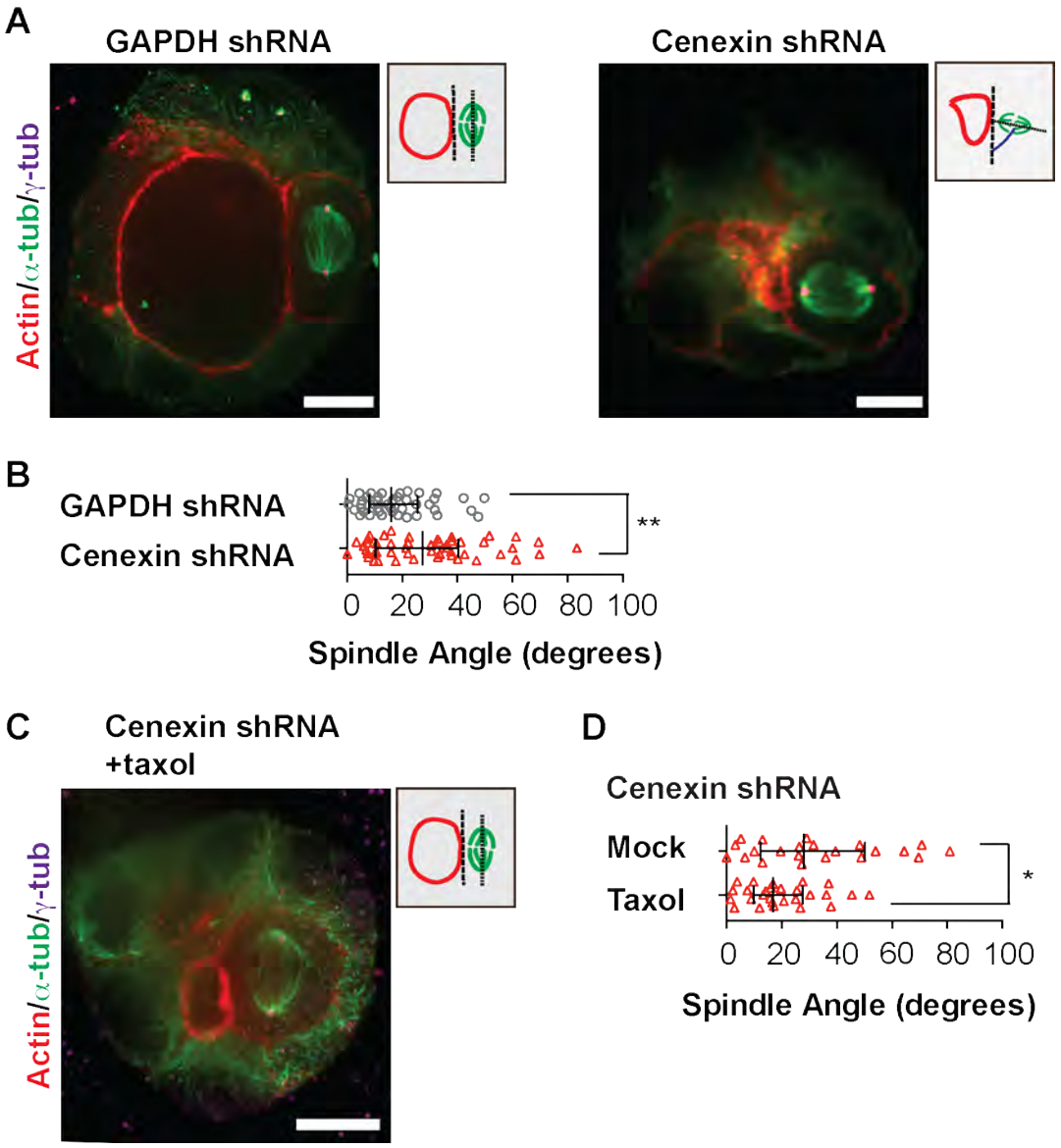

Figure 2.17 Cenexin-depletion leads to mitotic spindle tilting in 3-dimensional culture.

(A and C) 3D-cultured MDCK acini were stained for actin (red), centrosomes (γ-tubulin, magenta), and microtubules (α-tubulin, green). From the left to right are control cells (GAPDH-depleted), cenexin-depleted cells (A), and cenexin-depleted cells treated with taxol (C). Scale bar, 10 μm.

(B) Raw spindle angles measured from acini in (A). Spindle angles were measured in GAPDH-depleted cells (n=43), and cenexin-depleted cells (n=50). **, *p*-value<0.01.

(D) Raw spindle angles measured from cenexin-depleted acini treated with taxol (n=27) or without taxol (n=22) for 2 hours. *, *p*-value<0.05.

A

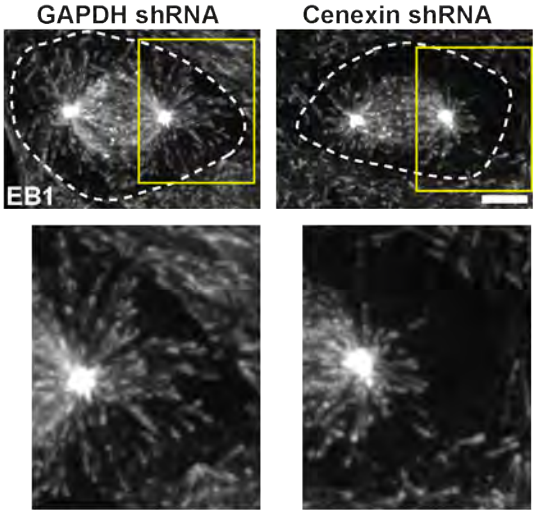

B

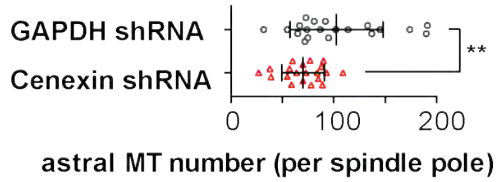

C

shRNA	astral MT Length (Mean ± SEM)
GAPDH	3.080 ± 0.03246, n=2032
Cenexin	2.574 ± 0.03629, n=1406

p<0.0001

D

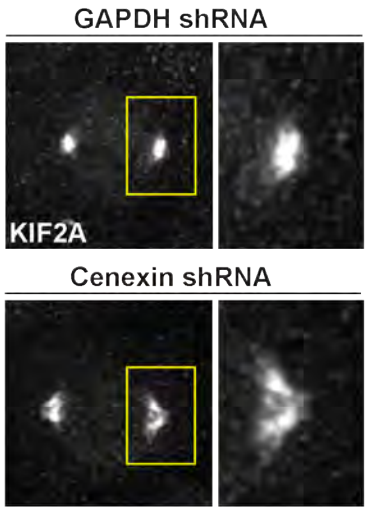

E

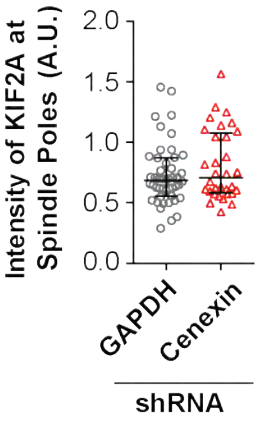

Figure 2.18 Cenexin depletion disrupts the organization of microtubules at spindle poles, and also causes astral microtubule defects.

(A and D) Metaphase spindles in MDCK cells were decorated with a plus-end microtubule marker, EB1 (A), or the minus-end microtubule marker, KIF2A (D). Dashed white line outlines edges of the cell (A). Insets taken from yellow box and magnified 2x to illustrate the shortening of astral microtubules (A) or the defocusing of KIF2A (D). Scale bar, 5 μm.

(B) Astral microtubule number per spindle pole was determined. Data are represented as mean ± SD of 20 spindle poles. **, *p*-value<0.01.

(C) Astral microtubule length was measured from spindle pole to microtubule tip labeled with EB1. n>10 cells/group. n-values listed in chart are the number of individual astral microtubules measured.

(E) The integrated intensity of KIF2A at spindle poles was measured for GAPDH-, and cenexin-depleted MDCK cells. Data are represented as mean ± SD of 46 poles in each group.

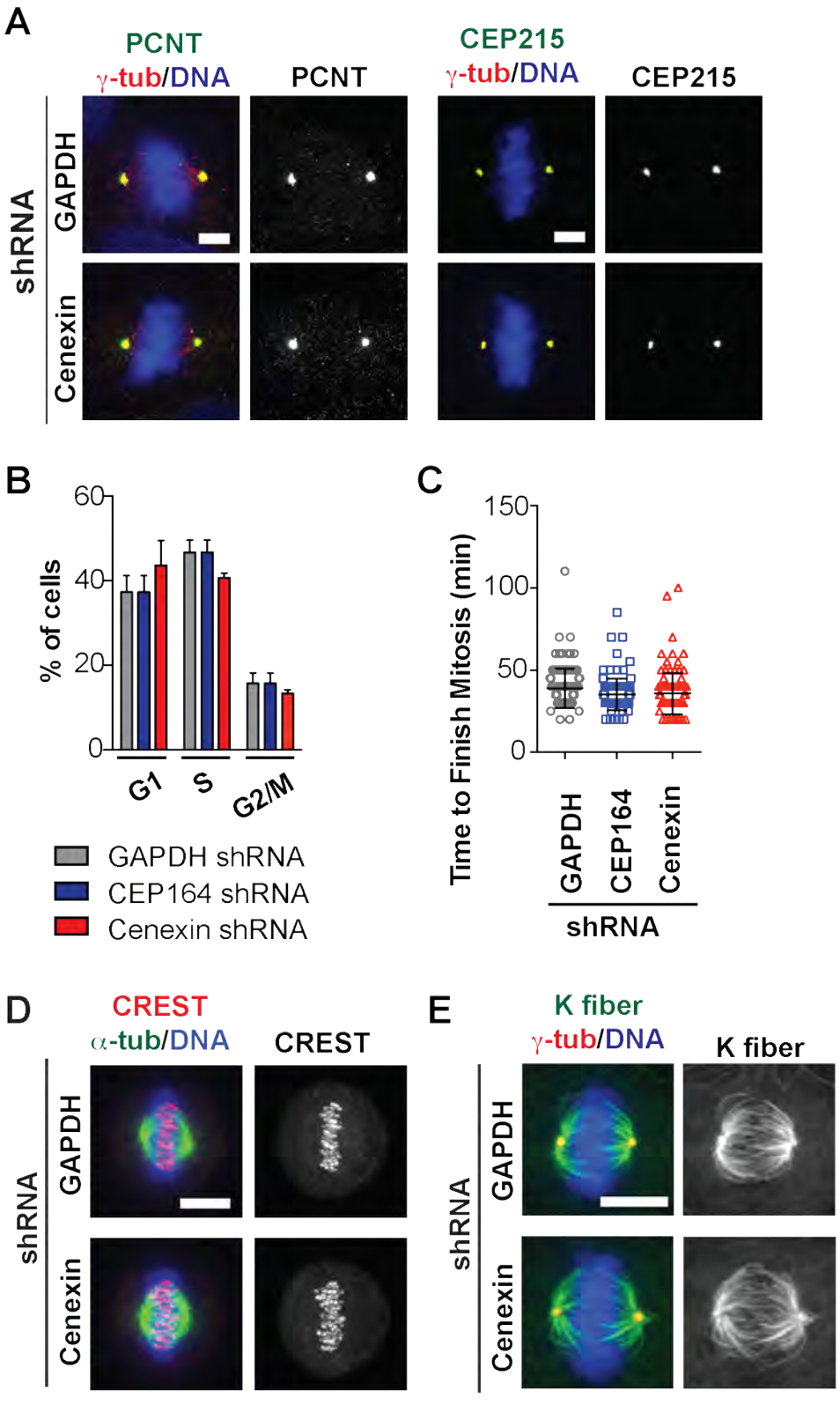
A
PCNT
γ-tub/DNA
PCNT
CEP215
γ-tub/DNA
CEP215
shRNA
GAPDH
Cenexin
B
% of cells
60
40
20
0
G1
S
G2/M
GAPDH shRNA
CEP164 shRNA
Cenexin shRNA
C
Time to Finish Mitosis (min)
150
100
50
0
GAPDH
CEP164
Cenexin
shRNA
D
CREST
α-tub/DNA
CREST
shRNA
GAPDH
Cenexin
E
K fiber
γ-tub/DNA
K fiber
shRNA
GAPDH
Cenexin

Figure 2.19 Cenexin depletion does not cause mitotic defects.

(A) The presence of PCNT (left) or CEP215 (right) at spindle poles was unchanged in cenexin-depleted U2OS cells. Spindle pole (γ-tubulin, red), PCNT or CEP215 (green). Scale bar, 5 μm.

(B) Cell cycle distribution was analyzed by propidium iodide (PI) staining and flow cytometry in MDCK cells depleted of GAPDH, CEP164, or cenexin. $2x10^4$ cells were analyzed in each group. The average percentage of cells at G1, S-phase, and G2/M are represented ± SD from 3 experiments.

(C) Time-lapse imaging was used to determine prophase to cytokinesis duration in MDCK cells depleted of GAPDH, CEP164, or cenexin. 100 cells were recorded in each group. Mean ± SD are shown.

(D) Cenexin-depletion does not affect chromosome congression during mitosis. Cells were stained for kinetochore (CREST, red), the mitotic spindle (α-tubulin, green), and DNA (DAPI, blue). Scale bar, 5 μm.

(E) Cenexin depletion does not affect kinetochore fibers in mitotic spindles. MDCK cells were placed on ice for 20 minutes before fixing. Cells were stained for kinetochore fibers (K fiber; α-tubulin, green), centrosomes (γ-tubulin, red), and DNA (DAPI, blue). Scale bar, 5 μm.

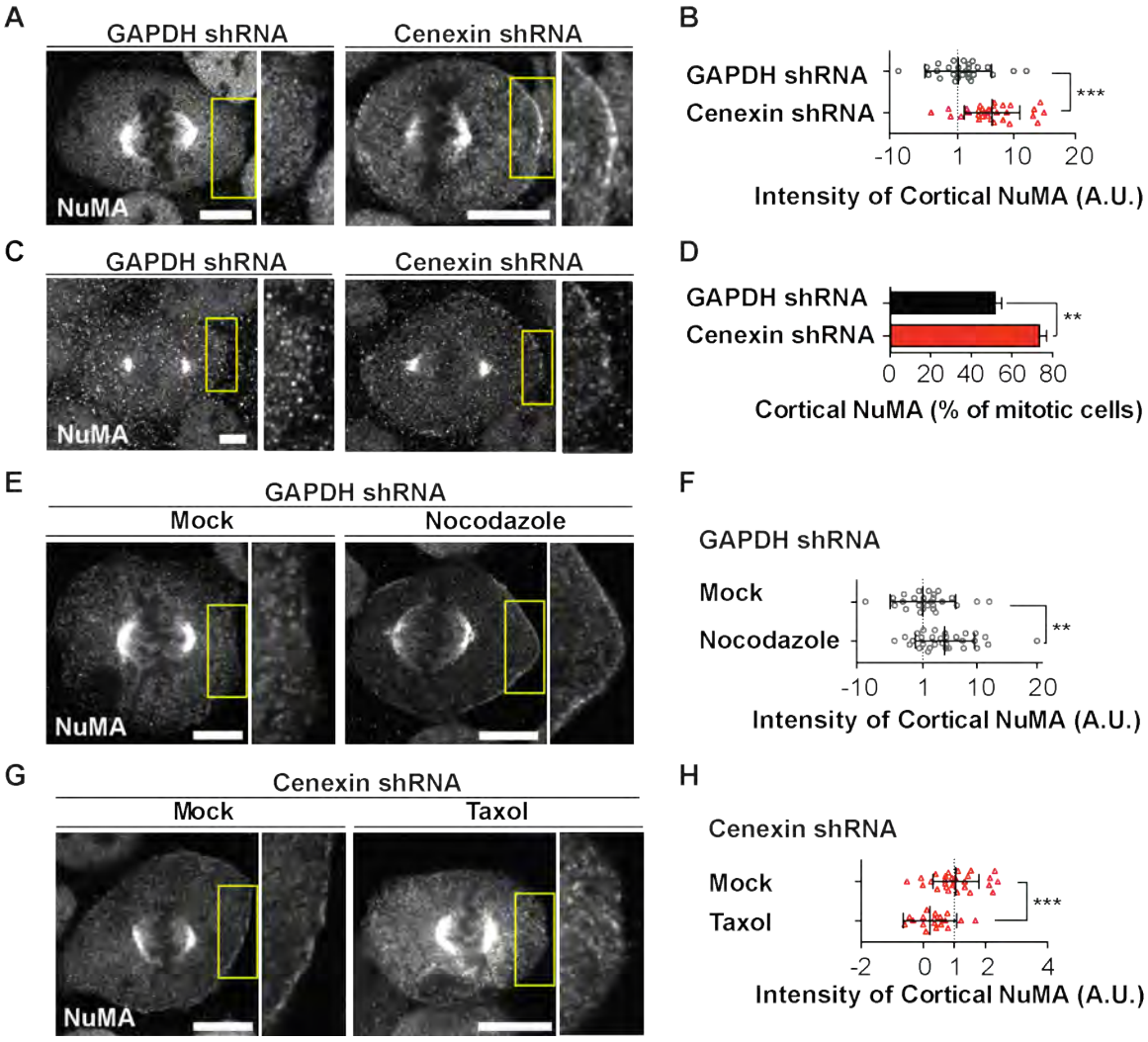
A
GAPDH shRNA
Cenexin shRNA
NuMA
B
GAPDH shRNA
Cenexin shRNA
***
-10 1 10 20
Intensity of Cortical NuMA (A.U.)
C
GAPDH shRNA
Cenexin shRNA
NuMA
D
GAPDH shRNA
Cenexin shRNA
**
0 20 40 60 80
Cortical NuMA (% of mitotic cells)
E
GAPDH shRNA
Mock
Nocodazole
NuMA
F
GAPDH shRNA
Mock
Nocodazole
**
-10 1 10 20
Intensity of Cortical NuMA (A.U.)
G
Cenexin shRNA
Mock
Taxol
NuMA
H
Cenexin shRNA
Mock
Taxol
***
-2 0 1 2 4
Intensity of Cortical NuMA (A.U.)

Figure 2.20 Cenexin depletion destabilizes astral microtubules and contributes to cortical NuMA mislocalization.

(A) Shown is a single z-section of NuMA staining in a metaphase U2OS cell depleted of GAPDH or cenexin. Scale bar, 5 μm. Inset taken from yellow box was magnified 2x to illustrate the increase in cortical NuMA after cenexin depletion compared to control (GAPDH shRNA).

(B) The cortical integrated intensity of NuMA (A) was measured in metaphase cells depleted of GAPDH or cenexin. Data are represented as mean ± SD of >28 cells/treatment. **, *p*-value<0.01.

(C) A single z-section is shown for metaphase MDCK cells depleted of GAPDH or cenexin were stained for NuMA. Scale bar, 5 μm. Insets taken from yellow box were magnified 2x to illustrate the increase in cortical NuMA with cenexin-loss compared to control (GAPDH-depleted cell).

(D) The percentage of mitotic cells with visible cortical NuMA localization in MDCK cells treated with cenexin- or GAPDH-shRNAs. Mean ± SEM. 30 cells/treatment were counted per n=3 experiments. **, *p*-value<0.01.

(E) GAPDH-depleted U2OS cells were treated with nocodazole and labeled for NuMA. Inset taken from yellow box was magnified 2x to illustrate the increase in cortical NuMA when disrupting astral microtubules with nocodazole treatment. Scale bar, 5 μm.

(G) Cenexin-depleted U2OS cells were treated with taxol and labeled for NuMA. Inset taken from yellow box was magnified 2x to illustrate the decrease in cortical NuMA when stabilizing astral microtubules with taxol treatment. Scale bar, 5 μm.

(F and H) The cortical integrated intensity of NuMA was measured in metaphase cells depleted of GAPDH (E), or cenexin (G). Data are represented as mean ± SD of >20 cells/treatment. **, *p*-value<0.01. ***, *p*-value<0.001.

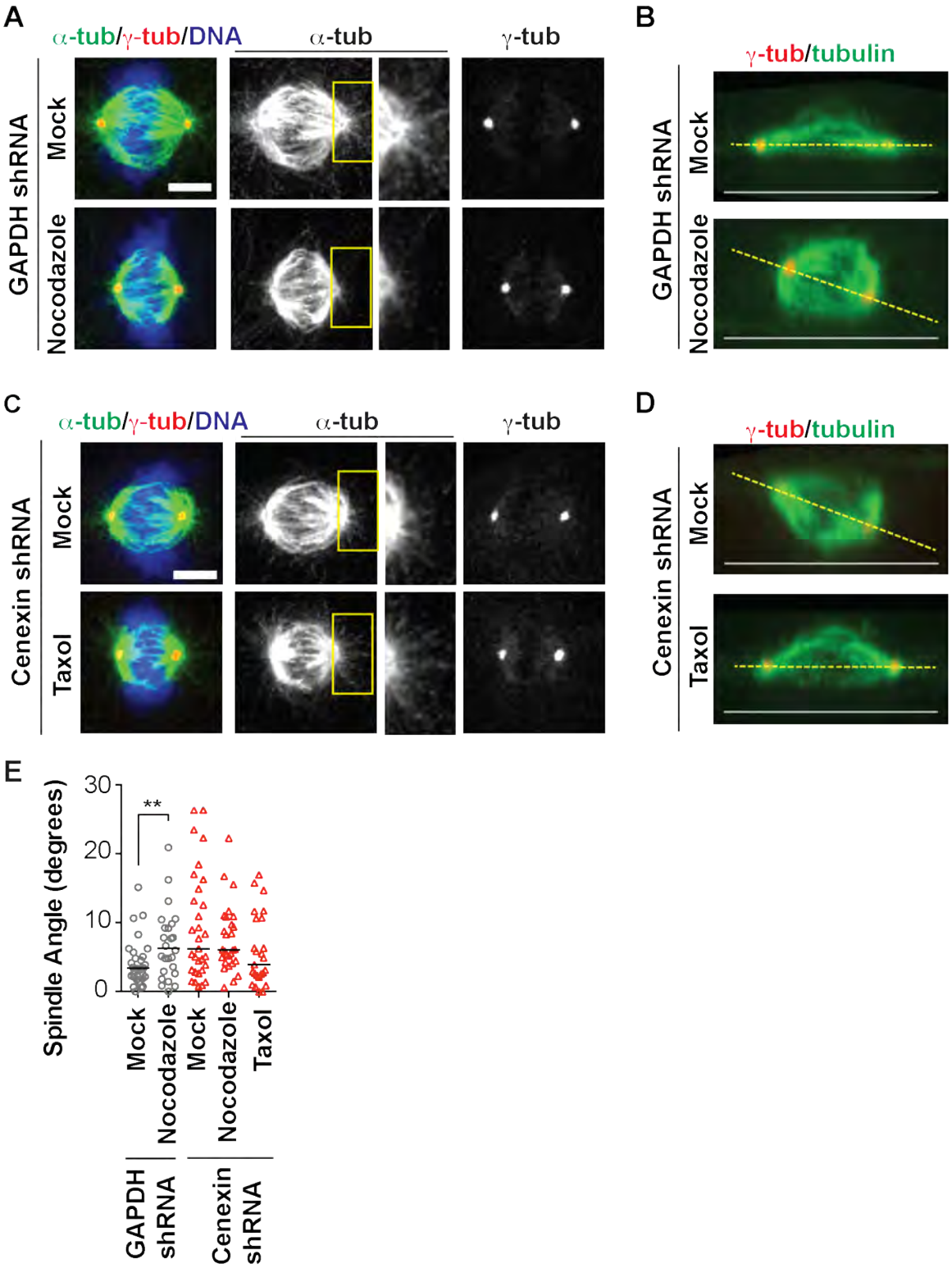
A
α-tub/γ-tub/DNA
α-tub
γ-tub
GAPDH shRNA
Mock
Nocodazole
B
γ-tub/tubulin
GAPDH shRNA
Mock
Nocodazole
C
α-tub/γ-tub/DNA
α-tub
γ-tub
Cenexin shRNA
Mock
Taxol
D
γ-tub/tubulin
Cenexin shRNA
Mock
Taxol
E
Spindle Angle (degrees)
30
20
10
0
**
Mock
Nocodazole
Mock
Nocodazole
Taxol
GAPDH shRNA
Cenexin shRNA

Figure 2.21 Stabilizing astral microtubules with taxol treatment rescues the spindle orientation defect in cenexin-depleted cells.

(A) Astral microtubules were disrupted with nocodazole treatment in control (GAPDH shRNA) U2OS cells, while the spindle and spindle poles were kept intact. Cells were fixed and stained for microtubules (α-tubulin, green), spindle poles (γ-tubulin, red), and DNA (DAPI, blue). Insets taken from yellow box were magnified 2x. Scale bar, 5 μm.

(B) Orthogonal view of metaphase U2OS cells treated with nocodazole, fixed, and stained for microtubules (α-tubulin, green), and spindle poles (γ-tubulin, red).

(C) Cenexin-depleted U2OS cells treated with taxol demonstrated an increase in astral microtubules. Cells were fixed and stained for microtubules (α-tubulin, green), spindle poles (γ-tubulin, red), and DNA (DAPI, blue). Insets taken from yellow box were magnified 2x. Scale bar, 5 μm.

(D) Orthogonal view of metaphase U2OS cells depleted of cenexin treated with taxol. Cells were fixed and stained for microtubules (α-tubulin, green), and spindle poles (γ-tubulin, red).

(E) Spindle angles were measured in GAPDH- and cenexin-depleted metaphase cells treated with or without taxol or nocodazole (as depicted). Data are represented as median of >25 cells/treatment. **, p-value<0.01.

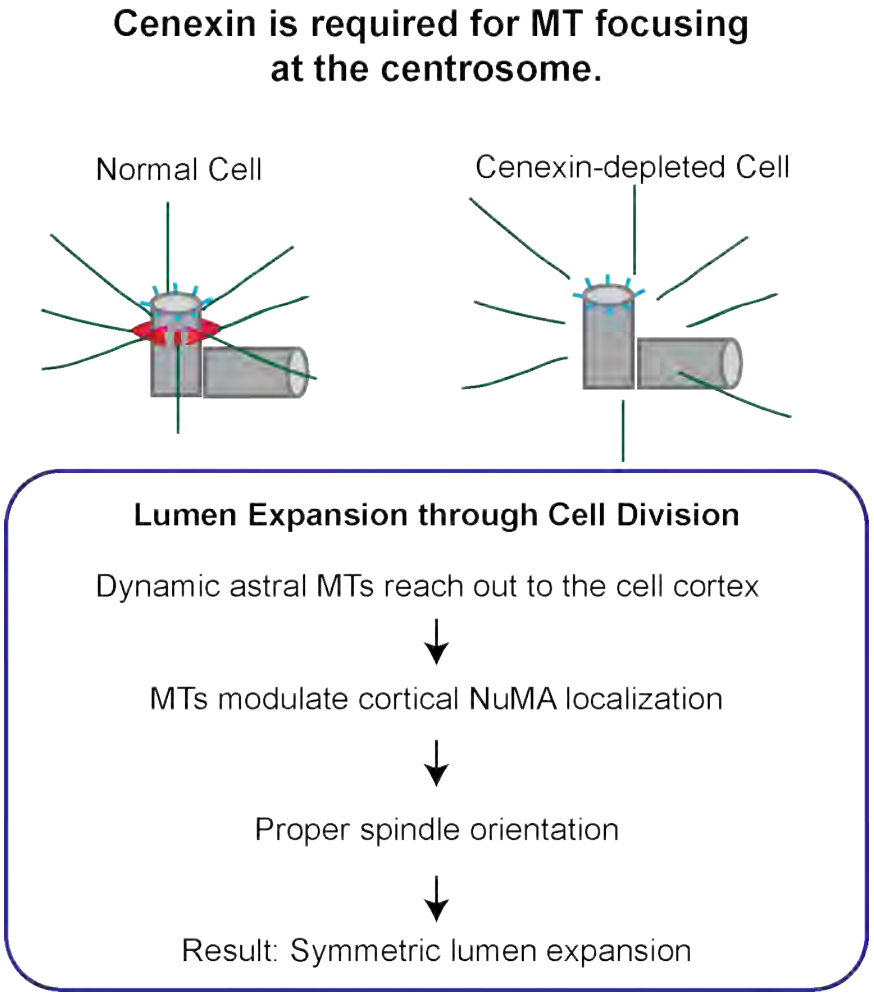

Figure 2.22 A model portraying cenexin functions in microtubule focusing and mitotic spindle orientation.

MATERIALS AND METHODS

Materials

The following primary antibodies were used for immunofluorescence staining or immunoblotting: rabbit anti-cenexin (Abcam and Proteintech), rabbit anti-CEP164 (from Dr. Erich Nigg, University of Basel, and Novus), goat anti-γ-tubulin (Santa Cruz), mouse anti-centrin (EMD Millipore), rat anti-α-tubulin (EMD Millipore), mouse anti-acetylated tubulin (Sigma-Aldrich), rabbit anti-NuMA (Abcam), mouse anti-E-cadherin (BD Biosciences), rabbit anti-PAR3 (EMD Millipore), rabbit anti-PKCζ (Santa Cruz), rabbit anti-pericentrin (Abcam), rabbit anti-CEP215 (Bethyl Laboratories). The following secondary antibodies were used for immunofluorescence staining: donkey anti-goat 568 (Invitrogen), donkey anti-rat DyLight 649, donkey anti-rabbit Alexa 647, donkey anti-mouse Alexa 647, donkey anti-rabbit Alexa 488, donkey anti-mouse DyLight 488 (Jackson ImmunoResearch Group). Nocodazole, taxol, and cytochalasin D were obtained from Sigma-Aldrich. GAPDH, cenexin (cenexin-1: V3LMM 507347; cenexin-2: V3LHS 336238, (Hehnly et al., 2012)), CEP164 (CEP164-1: V2LHS 96265; CEP164-2: V2LHS 232472), and pericentrin (V3LHS 368782) shRNAs were purchased from Open Biosystems (GE Dharmacon) and the UMMS RNAi Core Facility generated lentivirus for each. Human cenexin-GFP construct was from Dr. Kyung S Lee, National Cancer Institute (Soung et al., 2006), and we introduced two mutations on nucleotide 783-784 (AC➔GT) so that it was resistant to shRNA silencing.

Cell lines and culture

U2OS and MDCK cells were grown in Dulbecco's Modified Eagle Medium (Invitrogen) supplemented with 10% fetal bovine serum (Atlanta Biologicals) and 100 U/ml Penicillin-Streptomycin (Gibco). To establish cell lines depleted of a specific protein, lentiviruses expressing target gene shRNAs were incubated with cells for 24 hours in the presence of 4 µg/ml polybrene (Sigma). Puromycin (3 µg/ml) was used to select for transduced cells. The crossbow micropattern slides were from CYTOO (Mini CW-S-FN).

Nocodazole (M1401; Sigma) and taxol (T7191 and T7402; Sigma) were dissolved in DMSO. For nocodazole treatment, unless otherwise specified, the concentration of nocodazole was 100 nM. For taxol treatment, we titrated the working concentration by checking if it caused multiple spindle defects in mitosis. The working concentration that was used was 5-50 nM. For centrosome centering experiments with micropatterned slides , cells were seeded onto patterned slides and incubated for 2 hours for cell attachment. Cells were further incubated with nocodazole or taxol in serum-free medium for 2 hours before immunofluorescence staining.

Reverse transcription (RT-PCR) analysis

Total RNA was isolated from cells by using TRIzol reagent (Ambion), and 5 µg of RNA was converted into 100 µl of cDNA by using SuperScript II RT kit (Invitrogen). The following PCR primers were used to detect gene expression in MDCK cells: Actin, forward 5'-CAA AGC CAA CCG TGA GAA G-3', reverse 5'-CAG AGT CCA TGA CAA TAC CAG-3'; GAPDH, forward 5'-AAC ATC ATC CCT GCT TCC AC-3', reverse 5'-GAC

CAC CTG GTC CTC AGT GT-3’; cenexin primer-1, forward 5’-GCA TGT GCA ACT TGC TGA CA-3’, reverse 5’-TTC AGG ATG TCA GGC AGC TG-3’; cenexin primer-2, forward 5’-CAA CAT CGA GCG CAT CAA GG-3’, reverse 5’-GCT CAG CTT CTG CAG GAG AA-3’; CEP164 primer-1, forward 5’-GAC CCC CAA GTC TCA GGT TG-3’, reverse 5’-TTG TAT GCA GTG GAG AGG CG-3’; CEP164 primer-2, forward 5’-CCT GGA TGA GGC AGC ATT GA-3’, reverse 5’-AGT CAG CAG AGG GAG GAG AG-3’.

Immunofluorescence staining

Cells were seeded on glass coverslips (#1.5, Warner Instruments) and grown to sub-confluence for immunofluorescence confocal microscopy. Cells were then fixed (cold methanol) and stained as previous described (Chen et al., 2014; Delaval et al., 2011; Hehnly and Doxsey, 2014; Hehnly et al., 2012). Images were taken on a Perkin Elmer spinning disk confocal microscope: Zeiss Axiovert 200, Plan-Apochromat 100x/1.4 Oil DIC objective and Hamamatsu ORCA-ER camera. The entire cell was imaged at 0.2-µm step-intervals and displayed as maximum projections (MetaMorph, Molecular Device) unless otherwise specified. The fluorescence range of intensity was adjusted identically for each image series. For immunofluorescence staining of isolated centrosomes, centrosomes were prepared and stained according to our previous studies (Blomberg-Wirschell and Doxsey, 1998; Hehnly et al., 2012; Hung et al., 2015). For fluorescence intensity quantification at centrosomes/spindle poles, the integrated intensity was measured using a sum projection of the original stack followed by previously described methods (Chen et

al., 2014; Hehnly and Doxsey, 2014). The quantification of CEP128 (Figure 2.4B) was performed using maximum projections of the original stack due to a high degree of background staining. Orthogonal images of mitotic spindle were processed with Imaris software. For measuring spindle angles in 2-dimensional cultures, γ-tubulin staining was used to indicate spindle pole positions, and spindle angle measurements were carried out as previous described (Chen et al., 2014; Delaval et al., 2011; Hehnly and Doxsey, 2014). For measuring astral microtubule length by EB1 staining, Imaris software was used followed by a previously described method (Stout et al., 2011).

Three-dimensional acinus culture and staining

Modified from previously published methods (Debnath et al., 2003). MDCK cells were seeded in 2% matrigel (BD Biosciences) at 5 x 10^3 cells per well on matrigel pre-coated 8-well chamber slides (Thermo Scientific Nunc). After 36 to 48 hours, acini were fixed with 4% paraformaldehyde for 20 minutes, and permeablized with 0.5% Triton X-100 for 10 minutes at 4°C. Before blocking with 10% donkey serum for 2 hours, acini were rinsed with PBS twice. To stain target proteins, acini were incubated with primary antibodies overnight at 4°C. Acini were rinsed three times with PBS for 20 minutes each at room temperature and then incubated with rhodamine phalloidin or secondary antibodies for 1 hour. After a brief wash with PBS, acini were stained with DAPI and mounted in ProLong Gold Antifade reagent (Invitrogen). Images were taken at 0.2-μm intervals from the top to the bottom of the acinus on a spinning disk confocal microscope as described above. The number of lumina per acinus was quantified by actin staining. In addition, we

defined acini with less or equal to 5 cells, which undergo a maximum of 4 cell divisions, as the early stage of acinus formation. Acini with more than 5 cells were defined as acini in a later expansion stage. Matlab was used to generate scatter plots illustrating the number of lumina in acini.

For measuring spindle angles in acini, γ-tubulin staining was used to indicate spindle pole positions, and actin staining was used to indicate the apical lumen. Spindle angles in acini were then measured followed by a previously described method (Durgan et al., 2011). For the taxol treatment, cells were seeded and cultured as described above and incubated with taxol-containing medium for an additional 2 hours before performing immunofluorescence staining.

Transmission electron microscopy of mitotic spindle poles

Mitotic cells were collected by mitotic shake-off (Fox, 2004), and were fixed in 2.5% glutaraldehyde in PBS for 30 minutes. After post-fixation in 1% osmium tetroxide and embedding in SPI-Pon-Araldite, 150-nm sections were cut and examined with a Philips CM10 transmission electron microscope.

Migration assay

Cells were seeded at confluence with the ibidi culture-insert, and then cultured in serum-free conditions for 48 hours. After removing the inserts, cells were incubated in serum-containing medium for cell migration. Cells were then fixed at 2 - 6 hours and prepared for immunofluorescence staining. The percentage of centrosomes that reorient to a position

between the nucleus and the leading edge of the cell during migration was calculated as previously described (Gomes and Gundersen, 2006; Schliwa and Honer, 1993). For taxol treatment, cells were incubated with taxol containing medium after inducing cell migration.

CHAPTER III

DISCUSSION

The centrosome has been thought to control cell polarization and cell shape through its ability to organize microtubules. However, the mechanism of how centrosomal microtubules participate in cell polarization is not clear. Furthermore, there are different populations of microtubules at the centrosomes (nucleated and organized at PCM or anchored at the mother centriole appendages), which make it necessary to discern functions of microtubules from different populations. Previous results indicate the mother, but not the daughter, centriole is involved in centrosome positioning (Piel et al., 2000). In addition, PCM proteins have been shown to dramatically delocalize from the centrosome after cell division (Dictenberg et al., 1998; Khodjakov and Rieder, 1999; Piehl et al., 2004; Woodruff et al., 2014). Compared to mitosis, less microtubules are nucleated and organized at PCM, and the predominant microtubule population is subdistal appendage-anchored microtubules during interphase (Piehl et al., 2004). In addition, cells need to establish and maintain cell polarity at interphase. Therefore, we hypothesized that the microtubules anchored at mother centriole subdistal appendages are the main population of microtubules that contribute to cell polarity.

To determine the functions of anchored microtubules, we depleted cenexin, an essential structural protein of subdistal appendages (Ishikawa et al., 2005; Tanos et al., 2013), and studied the consequences in biological events, such as cell migration, cell division, and lumen formation. We found that cenexin depletion affects microtubule organization and stability during interphase and mitosis, and hence is required for centrosome reorientation during cell migration and spindle orientation during cell division (Hung et al., 2016). We proposed that subdistal appendages are required for microtubule

anchoring at the centrosome and anchored microtubules are more stable than microtubules at PCM.

Mother centriole subdistal appendage is involved in microtubule anchoring

Cenexin (cenexin-1, ODF2 isoform 9) is the major isoform of *ODF2* gene in somatic cells (Soung et al., 2006). Compared to its spliced variant, outer dense fibre protein 2 (ODF2) only found in sperm (Petersen et al., 1999), cenexin has a unique C-terminal extension, that is related to its functions of mother centriole localization, mitotic progression and ciliogenesis (Chang et al., 2013; Soung et al., 2006, 2009). We used the fact that cenexin depletion produces disruption of the subdistal appendage structure to study the roles of microtubules anchored at subdistal appendages. We found that depletion of cenexin disrupts microtubule organization at the centrosome/spindle pole. However, cenexin/ODF2 does not directly interact with microtubules (Donkor et al., 2004) and other proteins may mediate microtubule anchoring at subdistal appendages. Several proteins specifically localized at mother centriole subdistal appendages, ninein, CEP170 and trichoplein, have been proposed to anchor microtubules during interphase (Delgehyr et al., 2005; Guarguaglini et al., 2005; Ibi et al., 2011; Mogensen et al., 2000). Interestingly, these proteins are lost from centrosomes during metaphase (Casenghi et al., 2003; Guarguaglini et al., 2005), which is the mitotic stage where spindle orientation is determined. It will be of great interest to further examine the molecular components and mechanisms that directly anchor microtubules during interphase and mitosis.

Notably, other than spindle misorientation, we did not observe significant changes in cell cycling or mitotic progression in our cenexin-stably-depleted cells (Figure 2.19), while cenexin depletion causes G2/M arrest, apoptosis, and chromosome segregation defects in a previous study (Soung et al., 2006). This discrepancy may be due to different levels of cenexin reduction and assay time points after inducing cenexin depletion. More interestingly, slimier as the previous study (Soung et al., 2006), we also observed a decrease of PLK1 at the spindle poles. PLK1 is essential for centrosome maturation and mitotic progression, and the localization of PLK1 and appendage components to the centrosome/spindle pole is mutually dependent (Archambault and Glover, 2009; Guarguaglini et al., 2005; Kong et al., 2014; Lee and Rhee, 2011; Soung et al., 2006). In cenexin-depleted cells, the cell division defects related to loss of PLK1 from the spindle pole may be compensated by other mechanisms. However, PLK1 has been shown to negatively control the interaction between dynein and the NuMA/LGN complex, which generate the force to position the mitotic spindles (Kiyomitsu and Cheeseman, 2012). PLK1 might corporate with mother centriole appendage component to control spindle orientation through their direct interaction.

Microtubule organization during mitosis

The microtubule organization of interphase centrosomes is very different from mitotic spindles; long microtubules are almost evenly radiated out from interphase centrosomes while the spindle poles present astral microtubules and spindle microtubules. Furthermore, centrosomal microtubules are specifically stabilized and post-translationally

modified during centrosome reorientation in interphase, while astral microtubules are short-lived. It is possible that a separate mechanism regulates microtubule stability and organization during mitosis.

During mitosis, the centriole duplicates along with DNA replication, and the recruitment of mother centriole appendage proteins to the daughter centrosome, such as cenexin and CEP164, is the hallmark for centrosome maturation and required for cell division (Graser et al., 2007; Kong et al., 2014; Lange and Gull, 1995). This suggests that mother centriole appendages and components play an important role during mitosis. However, whether or not the appendage structure is present at centrosomes/spindle poles was an outstanding question. We collected mitotic cells for electron microscopy and found that appendages are present during mitosis (Figure 2.15A). Interestingly, there is a ~2-fold difference of cenexin localizing at the mother centrosome compared to the daughter centrosome, while the difference of CEP164 between two spindle poles was not as significant as cenexin (Figure 2.15B- 2.15D). To understand how the subdistal appendage organizes microtubules at spindle poles, it will be necessary to compare the localization of cenexin (subdistal appendages) between mother and daughter centrosomes.

Microtubule organization and microtubule dynamics

An interesting finding in our study is that disrupting microtubule minus-end organization at the centrosome/spindle pole affects microtubule stability in both interphase and mitotic cells (Figure 2.8, 2.12, 2.14, 2.18, and 2.21). In *in vitro* assays using pure tubulins, microtubules are polymerized and depolymerized both at the plus- and minus-

ends (Walker et al., 1988). On the contrary, the microtubule minus-ends attached to centrosomes exhibit a much more stable dynamics compared to free microtubules (Keating et al., 1997). Theoretically, centrosomal minus-ends can be protected by minus-end capping proteins. However, γ-tubulin ring complex (γTuRC) is the only identified minus-end binding protein at the centrosomes (Dammermann et al., 2003; Jiang and Akhmanova, 2011). Microtubule anchoring proteins on the subdistal appendages can be another minus-end capping protein, and therefore disrupting the subdistal appendage can expose the minus-ends and destabilize the microtubules.

Appendage-anchored and PCM-organized microtubules in spindle orientation

In our previous study, we found that disruption of a key PCM protein pericentrin causes spindle misorientation and astral microtubule defects (Chen et al., 2014). Pericentrin is a large coiled-coil protein, which serves as a scaffold for microtubule nucleation and centrosome/spindle pole organization (Chen et al., 2014; Dictenberg et al., 1998; Doxsey et al., 1994; Jurczyk et al., 2004; Li et al., 2000; Sillibourne et al., 2007; Takahashi et al., 2002; Young et al., 2000; Zimmerman et al., 2004). The reduction of microtubule nucleating activity and disruption of PCM organization can be the major contributors of the spindle orientation and astral microtubule defects in pericentrin mutation cells. However, depletion of pericentrin also disrupts the accumulation of subdistal appendage components centriolin and ninein at the centrosome/spindle pole. In addition, depletion of centriolin causes spindle misorientation, but is less severe compared to pericentrin depletion (Chen et al., 2014). These results suggest that both appendage anchored- and

PCM nucleated/organized- microtubules are essential for regulating spindle orientation. In the meanwhile, PCM component pericentrin and appendage components ninein and centriolin may be the link for these two populations of microtubules.

Conclusion

Currently, there are no known disease-related cenexin mutations, and this is likely due to the fundamental importance of the *ODF2* gene in cilium function. However, this study demonstrates subdistal appendages play a necessary role in cell migration and mitosis, reinforcing the importance of microtubule dynamics in these key biological events.

APPENDIX A

THE POSSIBLE ROLE OF MOTHER CENTRIOLE APPENDAGES IN REGULATING THE LOCALIZATION OF POLARITY PROTEINS

In our study of the function of cenexin in cell polarization and lumen formation, we observed no effects on cell polarity. This is consistent with a previous study of mice expressing truncated *Odf2* gene that shows defects in microtubule organization but normal cell polarization (Kunimoto et al., 2012; Tateishi et al., 2013). Interestingly, we often observed a weaker staining of apical polarity proteins (gp135, and PKCζ) at the surface of lumina in cenexin-depleted cells (Figure A.1A). To further quantify this phenotype, we picked control and cenexin-depleted acini with similar size and number of lumen, and measured the intensity of polarity proteins localized at the apical lumen surface (Figure A.1B and A.1C). The localization of gp135, and PKCζ at the apical lumen surface was slightly decreased in cenexin-depleted cells.

We hypothesize that cenexin depletion affects endosome trafficking, which participates in the delivery and recycling of polarity proteins (Blasky et al., 2015). We first checked whether the polarity proteins of our interest are cycled through endosomes. We isolated endosome membranes from interphase and mitotic cells, and then used immunoblotting to determine whether polarity proteins, NuMA and PKCζ, were co-precipitated with endosomal proteins, Rab11 and transferrin receptor (TFR). An interesting finding of our study was that the amount of endosome-loaded polarity protein NuMA, and PKCζ, increase during mitosis compared to interphase (Figure A.2). This result suggests there might be an active vesicle trafficking of polarity proteins during mitosis. In addition, this result implies that NuMA is delivered to the cell cortex through endosomes during mitosis, while the mechanism of how NuMA localizes to the cell cortex is not clear.

We were further interested in examining whether cenexin depletion affects endosome trafficking during mitosis. We estimated endosome trafficking by photo bleaching GFP-tagged Rab11-associated endosomes at the interphase centrosome or one of the spindle poles in metaphase cells, and monitoring the fluorescent recovery after photobleaching (FRAP). During both interphase and metaphase, the recovery is 2-fold faster in cenexin-depleted cells (Figure A.3). In a previous study, depletion of cenexin decreased the rate of transferrin cycling out of the cell and produced the accumulation of vesicles around the centrosome (Hehnly et al., 2012). Cenexin depletion may only affect vesicle trafficking out of the centrosome, but not have a profound effect on trafficking toward the centrosome. Therefore, we observed a net accumulation and faster recovery after photo bleaching in cenexin-depleted cells. Taken together, these results also suggest cenexin regulates endosome trafficking though a similar mechanism during mitosis and interphase.

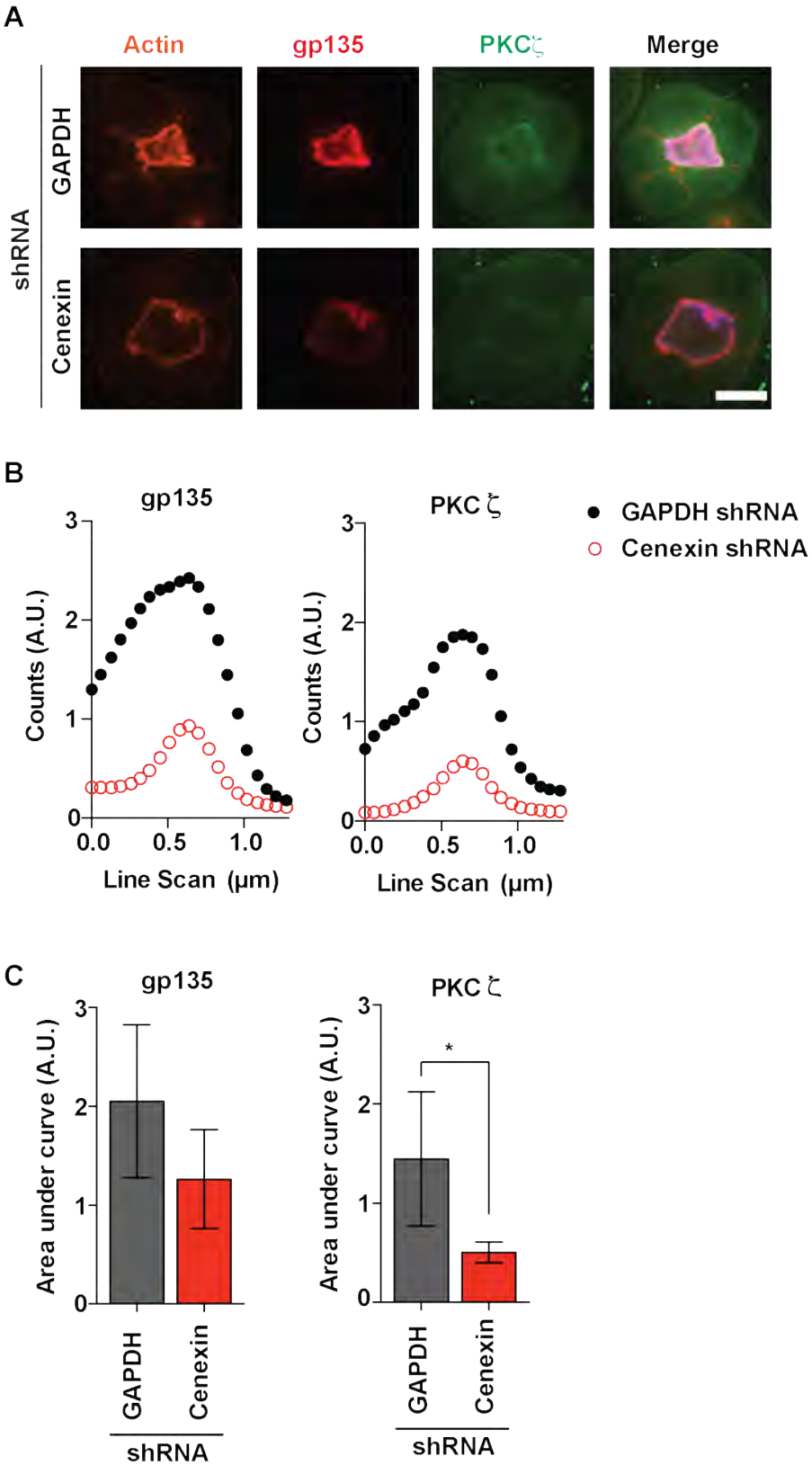
A
Actin
gp135
PKCζ
Merge
shRNA
GAPDH
Cenexin
B
gp135
PKC ζ
GAPDH shRNA
Cenexin shRNA
Counts (A.U.)
Line Scan (μm)
0.0
0.5
1.0
0
1
2
3
C
gp135
PKC ζ
Area under curve (A.U.)
*
GAPDH
Cenexin
shRNA

Figure A.1 Cenexin depletion reduces polarity proteins localizing at the apical lumen.

(A) 3D-cultured MDCK acini were stained for actin (orange), apical polarity proteins, gp135 (red) and PKCζ (green). A single confocal z-section at the center of the acinus is displayed. Scale bar, 10 μm.

(B) Line scans through apical lumen region of images in (A). Cenexin depletion reduces polarity proteins, gp135 (left) and PKCζ (right), localizing at the apical lumen.

(C) Quantification of area under curve in (B). Data are represented as mean ± SD of 5 lumina in each group. *, p-value<0.05.

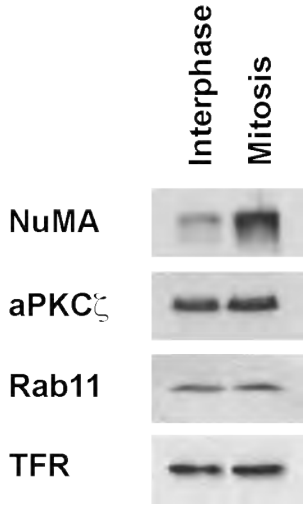

Figure A.2 Polarity proteins, NuMA and aPKCζ, traffic through endosomes in interphase and during mitosis.

U2OS cells were arrested in interphase by serum starvation, and mitotic cells were collected by mitotic shake-off. Endosome membranes were then isolated from interphase and mitotic cells according to our previous study (Hehnly and Doxsey, 2014). Immunoblot of isolated endosomes was used to examine whether polarity protein, NuMA and PKCζ, are loaded onto recycling endosome. Rab11 and transferrin receptor (TFR) are used for loading control and markers for endosomes.

A

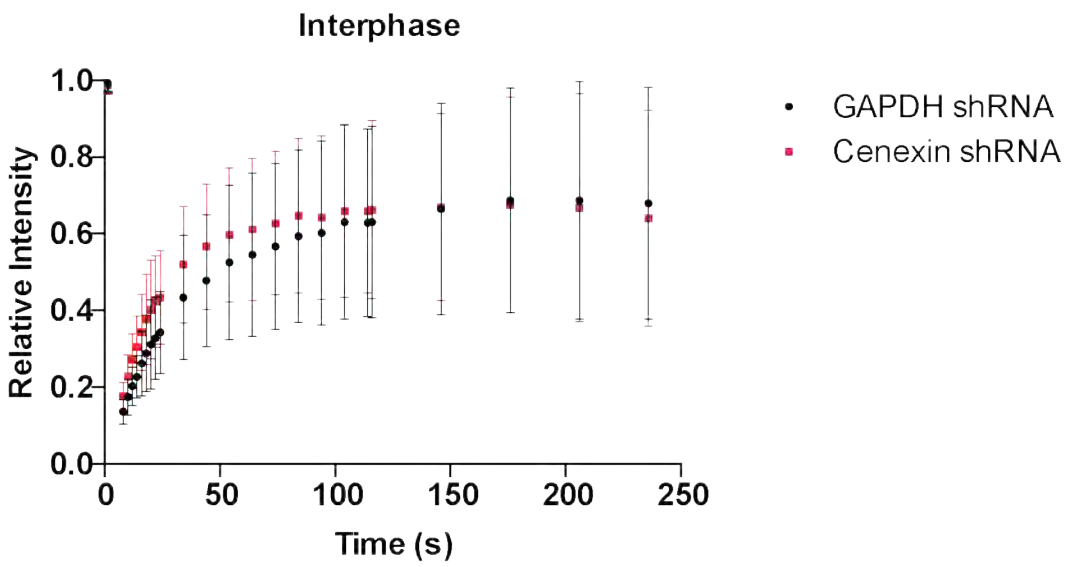

B

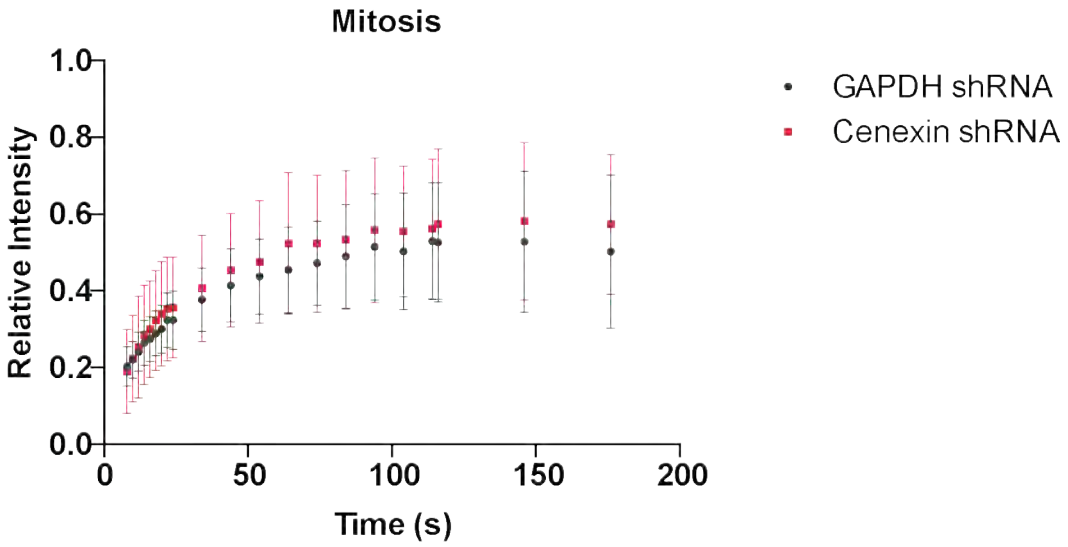

C

		thalf (sec)	
Interphase	Control	34.05 ± 3.545, n=16	***
	Cenexin shRNA	16.88 ± 2.476, n=17	
Mitosis	Control	34.54 ± 2.973, n=30	*
	Cenexin shRNA	24.41 ± 3.224, n=17	

Figure A.3 Endosomes traffic back to the centrosomes in a faster rate in cenexin-depleted cells compared to control.

Hela cells expressing FIP3-GFP were treated with GAPDH shRNA or cenexin shRNA and used for a fluorescent recovery after photobleaching (FRAP) experiment. It was performed with a Leica TCS SP5 II laser scanning confocal microscope using a 63x oil objective. The cells were imaging at 37°C, with 5% CO_2 using the Tokai Hit Stage Top Incubation System. The interphase centrosome (A) or one of the metaphase spindle pole was bleached at 100% laser intensity for 1 second twice. After photo bleaching, images were taken followed by every 2 seconds for 16 seconds, every 10 seconds for 90 seconds, and every 30 seconds for 2 minutes. The fluorescence intensity of the region of interest was normalize to the total cellular fluorescence intensity. $I= (T_0/I_0) * (I_t/T_t)$; T_0 and T_t is the total cellular fluorescence, and I_0 and I_t is the intensity of the centrosome/ spindle pole region.

(C) The half time of recovery (thalf) is calculated with the one-phase association equation using GraphPad Prism software. Data are represented as mean ± SE. *, *p*-value<0.05. ***, *p*-value<0.001.

REFERENCES

Ang, A.L., Fölsch, H., Koivisto, U., Pypaert, M., and Mellman, I. (2003). The Rab8 GTPase selectively regulates AP-1B–dependent basolateral transport in polarized Madin-Darby canine kidney cells. J. Cell Biol. *163*, 339–350.

Archambault, V., and Glover, D.M. (2009). Polo-like kinases: conservation and divergence in their functions and regulation. Nat Rev Mol Cell Biol *10*, 265–275.

Barros, T.P., Kinoshita, K., Hyman, A.A., and Raff, J.W. (2005). Aurora A activates D-TACC-Msps complexes exclusively at centrosomes to stabilize centrosomal microtubules. J. Cell Biol. *170*, 1039–1046.

Bettencourt-Dias, M., and Glover, D.M. (2007). Centrosome biogenesis and function: centrosomics brings new understanding. Nat. Rev. Mol. Cell Biol. *8*, 451–463.

Blasky, A.J., Mangan, A., and Prekeris, R. (2015). Polarized protein transport and lumen formation during epithelial tissue morphogenesis. Annu. Rev. Cell Dev. Biol. *31*, 575–591.

Blomberg-Wirschell, M., and Doxsey, S.J. (1998). Rapid isolation of centrosomes. Methods Enzymol. *298*, 228–238.

Bornens, M. (2002). Centrosome composition and microtubule anchoring mechanisms. Curr. Opin. Cell Biol. *14*, 25–34.

Bornens, M. (2012). The Centrosome in Cells and Organisms. Science (80-.). *335*, 422–426.

Bryant, D.M., and Mostov, K.E. (2008). From cells to organs : building polarized tissue. Nat. Rev. Mol. Cell Biol. *9*, 887–901.

Casenghi, M., Meraldi, P., Weinhart, U., Duncan, P.I., Körner, R., and Nigg, E.A. (2003). Polo-like kinase 1 regulates Nlp, a centrosome protein involved in microtubule nucleation. Dev. Cell *5*, 113–125.

Chang, J., Seo, S.G., Lee, K.H., Nagashima, K., Bang, J.K., Kim, B.Y., Erikson, R.L., Lee, K.-W., Lee, H.J., Park, J.-E., et al. (2013). Essential role of Cenexin1, but not Odf2, in ciliogenesis. Cell Cycle *12*, 655–662.

Chen, C.-T., Hehnly, H., Yu, Q., Farkas, D., Zheng, G., Redick, S.D., Hung, H.-F., Samtani, R., Jurczyk, A., Akbarian, S., et al. (2014). A Unique Set of Centrosome Proteins Requires Pericentrin for Spindle-Pole Localization and Spindle Orientation. Curr. Biol. *24*, 2327–2334.

Cook, T.A., Nagasaki, T., and Gundersen, G.G. (1998). Rho guanosine triphosphatase mediates the selective stabilization of microtubules induced by lysophosphatidic acid. J. Cell Biol. *141*, 175–185.

Dabbeekeh, J.T.S., Faitar, S.L., Dufresne, C.P., and Cowell, J.K. (2007). The EVI5 TBC domain provides the GTPase-activating protein motif for RAB11. Oncogene *26*, 2804–2808.

Dammermann, A., and Merdes, A. (2002). Assembly of centrosomal proteins and microtubule organization depends on PCM-1. J. Cell Biol. *159*, 255–266.

Dammermann, A., Desai, A., and Oegema, K. (2003). The minus end in sight. Curr. Biol.

13, 614–624.

Debnath, J., Muthuswamy, S.K., and Brugge, J.S. (2003). Morphogenesis and oncogenesis of MCF-10A mammary epithelial acini grown in three-dimensional basement membrane cultures. Methods *30*, 256–268.

Delaval, B., Bright, A., Lawson, N.D., and Doxsey, S. (2011). The cilia protein IFT88 is required for spindle orientation in mitosis. Nat. Cell Biol. *13*, 461–468.

Delgehyr, N., Sillibourne, J., and Bornens, M. (2005). Microtubule nucleation and anchoring at the centrosome are independent processes linked by ninein function. J. Cell Sci. *118*, 1565–1575.

Dictenberg, J., Zimmerman, W., Sparks, C., Young, A., Vidair, C., Zheng, Y., Carrington, W., Fay, F.S., and Doxsey, S. (1998). Pericentrin and gama-tubulin form a protein complex and are organized into a novel lattice at the centrosome. J. Cell Biol. *141*, 163–174.

Donkor, F.F., Mönnich, M., Czirr, E., Hollemann, T., and Hoyer-Fender, S. (2004). Outer dense fibre protein 2 (ODF2) is a self-interacting centrosomal protein with affinity for microtubules. J. Cell Sci. *117*, 4643–4651.

Doxsey, S. (2001). Re-evaluating centrosome function. Nat. Rev. Mol. Cell Biol. *2*, 688–698.

Doxsey, S.J., Steln, P., Evans, L., Calarco, P.D., and Kirschnefi, M. (1994). Pericentrin , a highly conserved centrosome protein involved in microtubule organization. Cell *76*, 639–650.

Durgan, J., Kaji, N., Jin, D., and Hall, A. (2011). Par6B and atypical PKC regulate mitotic spindle orientation during epithelial morphogenesis. J. Biol. Chem. *286*, 12461–12474.

Elric, J., and Etienne-Manneville, S. (2014). Centrosome positioning in polarized cells: common themes and variations. Exp. Cell Res. *328*, 240–248.

Faitar, S.L., Dabbeekeh, J.T.S., Ranalli, T.A., and Cowell, J.K. (2005). EVI5 is a novel centrosomal protein that binds to a- and g-tubulin. Genomics *86*, 594–605.

Fırat-karalar, E.N., and Stearns, T. (2014). The centriole duplication cycle. Philos. Trans. R. Soc. Lond. B. Biol. Sci. *369*, 1–10.

Fox, M.H. (2004). Methods for synchronizing mammalian cells. Methods Mol. Biol. *241*, 11–16.

Ganem, N.J., and Compton, D. (2004). The KinI kinesin Kif2a is required for bipolar spindle assembly through a functional relationship with MCAK. J. Cell Biol. *166*, 473–478.

Gasic, I., Nerurkar, P., and Meraldi, P. (2015). Centrosome age regulates kinetochore–microtubule stability and biases chromosome mis-segregation. Elife *4*, e07909.

Gillies, T.E., and Cabernard, C. (2011). Cell division orientation in animals. Curr. Biol. *21*, 599–609.

Gomes, E.R., and Gundersen, G.G. (2006). Real-time centrosome reorientation during fibroblast migration. Methods Enzymol. *406*, 579–592.

Graser, S., Stierhof, Y.D., Lavoie, S., Gassner, O., Lamla, S., Le Clech, M., and Nigg, E.

(2007). Cep164, a novel centriole appendage protein required for primary cilium formation. J. Cell Biol. *179*, 321–330.

Gromley, A., Jurczyk, A., Sillibourne, J., Halilovic, E., Mogensen, M., Groisman, I., Blomberg, M., and Doxsey, S. (2003). A novel human protein of the maternal centriole is required for the final stages of cytokinesis and entry into S phase. J. Cell Biol. *161*, 535–545.

Gromley, A., Yeaman, C., Rosa, J., Redick, S., Chen, C., Mirabelle, S., Guha, M., Sillibourne, J., and Doxsey, S. (2005). Centriolin Anchoring of Exocyst and SNARE Complexes at the Midbody Is Required for Secretory-Vesicle-Mediated Abscission. Cell *123*, 75–87.

Guarguaglini, G., Duncan, P.I., Stierhof, Y.D., Holmstro, T., Duensing, S., and Nigg, E.A. (2005). The Forkhead-associated Domain Protein Cep170 Interacts with Polo-like Kinase 1 and Serves as a Marker for Mature Centrioles. Mol. Biol. Cell *16*, 1095–1107.

Hao, Y., Du, Q., Chen, X., Zheng, Z., Balsbaugh, J.L., Maitra, S., Shabanowitz, J., Hunt, D.F., and MacAra, I.G. (2010). Par3 controls epithelial spindle orientation by aPKC-mediated phosphorylation of apical pins. Curr. Biol. *20*, 1809–1818.

Hehnly, H., and Doxsey, S. (2014). Rab11 Endosomes Contribute to Mitotic Spindle Organization and Orientation. Dev. Cell *28*, 497–507.

Hehnly, H., Chen, C.T., Powers, C.M., Liu, H.L., and Doxsey, S. (2012). The centrosome regulates the Rab11- dependent recycling endosome pathway at appendages of the

mother centriole. Curr. Biol. *22*, 1944–1950.

Hehnly, H., Hung, H.-F., and Doxsey, S. (2013). One among many: ODF2 isoform 9, a.k.a. Cenexin-1, is required for ciliogenesis. Cell Cycle *12*, 1021.

Hehnly, H., Canton, D., Bucko, P., Langeberg, L.K., Ogier, L., Gelman, I., Santana, L.F., Wordeman, L., and Scott, J.D. (2015). A mitotic kinase scaffold depleted in testicular seminomas impacts spindle orientation in germ line stem cells. Elife *4*, e09384.

Henry, L., and Sheff, D.R. (2008). Rab8 Regulates Basolateral Secretory , But Not Recycling , Traffic at the Recycling Endosome. Mol. Biol. Cell *19*, 2059–2068.

Holy, T.E., Dogterom, M., Yurke, B., and Leibler, S. (1997). Assembly and positioning of microtubule asters in microfabricated chambers. Proc. Natl. Acad. Sci. *94*, 6228–6231.

Hung, H.-F., Hehnly, H., and Doxsey, S. (2015). Methods to analyze novel liaisons between endosomes and centrosomes. Methods Cell Biol. *130*, 47–58.

Hung, H.F., Hehnly, H., and Doxsey, S. (2016). The mother centriole appendage protein cenexin modulates lumen formation through spindle orientation. Curr. Biol. *26*, 793–801.

Ibi, M., Zou, P., Inoko, A., Shiromizu, T., Matsuyama, M., Hayashi, Y., Enomoto, M., Mori, D., Hirotsune, S., Kiyono, T., et al. (2011). Trichoplein controls microtubule anchoring at the centrosome by binding to Odf2 and ninein. J. Cell Sci. *124*, 857–864.

Ishikawa, H., Kubo, A., Tsukita, S., and Tsukita, S. (2005). Odf2-deficient mother centrioles lack distal/subdistal appendages and the ability to generate primary cilia. Nat. Cell Biol. *7*, 517–524.

Jaffe, A.B., Kaji, N., Durgan, J., and Hall, A. (2008). Cdc42 controls spindle orientation to position the apical surface during epithelial morphogenesis. J. Cell Biol. *183*, 625–633.

Jakobsen, L., Vanselow, K., Skogs, M., Toyoda, Y., Lundberg, E., Poser, I., Falkenby, L.G., Bennetzen, M., Westendorf, J., Nigg, E.A., et al. (2011). Novel asymmetrically localizing components of human centrosomes identified by complementary proteomics methods. EMBO J. *30*, 1520–1535.

Jiang, K., and Akhmanova, A. (2011). Microtubule tip-interacting proteins: A view from both ends. Curr. Opin. Cell Biol. *23*, 94–101.

Jurczyk, A., Gromley, A., Redick, S., San Agustin, J., Witman, G., Pazour, G.J., Peters, D.J.M., and Doxsey, S. (2004). Pericentrin forms a complex with intraflagellar transport proteins and polycystin-2 and is required for primary cilia assembly. J. Cell Biol. *166*, 637–643.

Keating, T.J., Peloquin, J.G., Rodionov, V.I., Momcilovic, D., and Borisy, G.G. (1997). Microtubule release from the centrosome. Proc. Natl. Acad. Sci. U. S. A. *94*, 5078–5083.

Khodjakov, A., and Rieder, C.L. (1999). The Sudden Recruitment of g-Tubulin to the Centrosome at the Onset of Require Microtubules. J. Cell Biol. *146*, 585–596.

Kiyomitsu, T., and Cheeseman, I.M. (2012). Chromosome- and spindle-pole-derived signals generate an intrinsic code for spindle position and orientation. Nat. Cell Biol. *14*, 311–317.

Kollman, J.M., Merdes, A., Mourey, L., and Agard, D. (2011). Microtubule nucleation by γ-tubulin complexes. Nat. Rev. Mol. Cell Biol. *12*, 709–721.

Kong, D., Farmer, V., Shukla, A., James, J., Gruskin, R., Kiriyama, S., and Loncarek, J. (2014). Centriole maturation requires regulated Plk1 activity during two consecutive cell cycles. J. Cell Biol. *206*, 855–865.

Kotak, S., and Gönczy, P. (2013). Mechanisms of spindle positioning: cortical force generators in the limelight. Curr. Opin. Cell Biol. *25*, 741–748.

Kotak, S., Busso, C., and Gönczy, P. (2014). NuMA interacts with phosphoinositides and links the mitotic spindle with the plasma membrane. EMBO J. *33*, 1815–1830.

Kunimoto, K., Yamazaki, Y., Nishida, T., Shinohara, K., Ishikawa, H., Hasegawa, T., Okanoue, T., Hamada, H., Noda, T., Tamura, A., et al. (2012). Coordinated ciliary beating requires Odf2-mediated polarization of basal bodies via basal feet. Cell *148*, 189–200.

Lange, B.M.H., and Gull, K. (1995). A molecular marker for centriole maturation in the mammalian cell cycle. J. Cell Biol. *130*, 919–927.

Lee, K., and Rhee, K. (2011). PLK1 phosphorylation of pericentrin initiates centrosome maturation at the onset of mitosis. J. Cell Biol. *195*, 1093–1101.

Li, Q., Hansen, D., Killilea, A., Joshi, H., Palazzo, R.E., and Balczon, R. (2000).

Kendrin/pericentrin-B, a centrosome protein with homology to pericentrin that complexes with PCM-1. J. Cell Sci. *114*, 797–809.

Luxton, G.G., and Gundersen, G.G. (2011). Orientation and function of the nuclear–centrosomal axis during cell migration. Curr. Opin. Cell Biol. *23*, 579–588.

Luxton, G.W.G., Gomes, E.R., Folker, E.S., Worman, H., Luxton, G.W.G., Gomes, E.R., Folker, E.S., and Worman, H. (2011). TAN lines:a novel nuclear envelope structure involved in nuclear positioning. Nucleus *2*, 173–181.

Magdalena, J., Millard, T.H., and Machesky, L.M. (2003). Microtubule involvement in NIH 3T3 Golgi and MTOC polarity establishment. J. Cell Sci. *116*, 743–756.

Martin-belmonte, F., and Perez-moreno, M. (2011). Epithelial cell polarity , stem cells and cancer. Nat. Rev. Cancer *12*, 23–38.

McCaffrey, L.M., and Macara, I.G. (2011). Epithelial organization, cell polarity and tumorigenesis. Trends Cell Biol. *21*, 727–735.

Mogensen, M.M., Malik, A., Piel, M., Bouckson-Castaing, V., and Bornens, M. (2000). Microtubule minus-end anchorage at centrosomal and non-centrosomal sites: the role of ninein. J. Cell Sci. *113*, 3013–3023.

Monteleon, C.L., and D'Souza-Schorey, C. (2012). Modeling disease using three dimensional cell culture: multi-lumen and inverted cyst phenotypes. Front. Biosci. *4*, 2864–2871.

Muthuswamy, S.K., and Xue, B. (2012). Cell Polarity as a Regulator of Cancer Cell Behavior Plasticity. Annu. Rev. Cell Dev. Biol. *28*, 599–628.

Overeem, A.W., Bryant, D.M., and Ijzendoorn, S.C.D. Van (2015). Mechanisms of apical – basal axis orientation and epithelial lumen positioning. Trends Cell Biol. *25*, 476–485.

Palazzo, A., Cook, T., Alberts, A., and Gundersen, G. (2001). mDia mediates Rho-regulated formation and orientation of stable microtubules. Nat. Cell Biol. *3*, 723–729.

Palazzo, A., Ackerman, B., and Gundersen, G.G. (2003). Cell biology: Tubulin acetylation and cell motility. Nature *421*, 230.

Petersen, C., Füzesi, L., and Hoyer-Fender, S. (1999). Outer dense fibre proteins from human sperm tail: Molecular cloning and expression analyses of two cDNA transcripts encoding proteins of ~70 kDa. Mol. Hum. Reprod. *5*, 627–635.

Piehl, M., Tulu, U.S., Wadsworth, P., and Cassimeris, L. (2004). Centrosome maturation: measurement of microtubule nucleation throughout the cell cycle by using GFP-tagged EB1. Proc. Natl. Acad. Sci. U. S. A. *101*, 1584–1588.

Piel, M., Meyer, P., Khodjakov, A., Rieder, C.L., and Bornens, M. (2000). The Respective Contributions of the Mother and Daughter Centrioles to Centrosome Activity and Behavior in Vertebrate Cells. J. Cell Biol. *149*, 317–329.

Rodriguez-Boulan, E., and Macara, I.G. (2014). Organization and execution of the epithelial polarity programme. Nat. Rev. Mol. Cell Biol. *15*, 225–242.

Rodríguez-Fraticelli, A., Gálvez-Santisteban, M., and Martín-Belmonte, F. (2011). Divide and polarize : recent advances in the molecular mechanism regulating

epithelial tubulogenesis. Curr. Opin. Cell Biol. *23*, 638–646.

Rodríguez-Fraticelli, A.E., Auzan, M., Alonso, M.A., Bornens, M., and Martín-Belmonte, F. (2012). Cell confinement controls centrosome positioning and lumen initiation during epithelial morphogenesis. J. Cell Biol. *198*, 1011–1023.

Salaycik, K.J., Fagerstrom, C.J., Murthy, K., Tulu, U.S., and Wadsworth, P. (2005). Quantification of microtubule nucleation, growth and dynamics in wound-edge cells. J. Cell Sci. *118*, 4113–4122.

Sato, T., Mushiake, S., Kato, Y., Sato, K., Sato, M., Takeda, N., Ozono, K., Miki, K., Kubo, Y., Tsuji, A., et al. (2007). The Rab8 GTPase regulates apical protein localization in intestinal cells. Nature *448*, 366–369.

Sato, T., Iwano, T., Kunii, M., Matsuda, S., Mizuguchi, R., and Jung, Y. (2014). Rab8a and Rab8b are essential for several apical transport pathways but insufficient for ciliogenesis. J. Cell Sci. *127*, 422–431.

Schliwa, M., and Honer, B. (1993). Microtubules, centrosomes and intermediate filaments in directed cell movement. Trends Cell Biol. *3*, 377–380.

Schmeichel, K.L., and Bissell, M.J. (2003). Modeling tissue-specific signaling and organ function in three dimensions. J. Cell Sci. *116*, 2377–2388.

Schmidt, K.N., Kuhns, S., Neuner, A., Hub, B., Zentgraf, H., and Pereira, G. (2012). Cep164 mediates vesicular docking to the mother centriole during early steps of ciliogenesis. J. Cell Biol. *199*, 1083–1101.

Schmoranzer, J., Fawcett, J.P., Segura, M., Tan, S., Vallee, R.B., Pawson, T., and

Gundersen, G.G. (2009). Par3 and Dynein Associate to Regulate Local Microtubule Dynamics and Centrosome Orientation during Migration. Curr. Biol. *19*, 1065–1074.

Schrøder, J., Rogowski, M., Jakobsen, L., Vanselow, K., Geimer, S., Pedersen, L., and Andersen, J. (2012). Identification and characterization of two novel centriolar appendage component proteins. Cilia *1*, 44.

Sillibourne, J.E., Delaval, B., Redick, S., Sinha, M., and Doxsey, S. (2007). Chromatin Remodeling Proteins Interact with Pericentrin to Regulate Centrosome Integrity. Mol. Biol. Cell *18*, 986–994.

Soung, N.-K., Kang, Y.H., Kim, K., Kamijo, K., Yoon, H., Seong, Y.-S., Kuo, Y.-L., Miki, T., Kim, S.R., Kuriyama, R., et al. (2006). Requirement of hCenexin for proper mitotic functions of polo-like kinase 1 at the centrosomes. Mol. Cell. Biol. *26*, 8316–8335.

Soung, N.-K.K., Park, J.-E.E., Yu, L.-R.R., Lee, K.S.H.S.H., Lee, J.-M.M., Bang, J.K., Veenstra, T.D., Rhee, K., and Lee, K.S.H.S.H. (2009). Plk1-Dependent and -Independent Roles of an ODF2 Splice Variant, hCenexin1, at the Centrosome of Somatic Cells. Dev. Cell *16*, 539–550.

Stenmark, H. (2009). Rab GTPases as coordinators of vesicle traffic. Nat. Publ. Gr. *10*, 513–525.

Stout, J.R., Yount, A.L., Powers, J. a, Leblanc, C., Ems-McClung, S.C., and Walczak, C.E. (2011). Kif18B interacts with EB1 and controls astral microtubule length

during mitosis. Mol. Biol. Cell *22*, 3070–3080.

Sütterlin, C., and Colanzi, A. (2010). The Golgi and the centrosome: building a functional partnership. J. Cell Biol. *188*, 621–628.

Takahashi, M., Yamagiwa, A., Nishimura, T., Mukai, H., and Ono, Y. (2002). Centrosomal Proteins CG-NAP and Kendrin Provide Microtubule Nucleation Sites by Anchoring gamma -Tubulin Ring Complex. Mol. Biol. Cell *13*, 3235–3245.

Tang, N., and Marshall, W.F. (2012). Centrosome positioning in vertebrate development. J. Cell Sci. *125*, 4951–4961.

Tanos, B.E., Yang, H.J., Soni, R., Wang, W.J., Macaluso, F.P., Asara, J.M., and Tsou, M.B.F.B. (2013). Centriole distal appendages promote membrane docking, leading to cilia initiation. Genes Dev. *27*, 163–168.

Tateishi, K., Yamazaki, Y., Nishida, T., Watanabe, S., Kunimoto, K., Ishikawa, H., and Tsukita, S. (2013). Two appendages homologous between basal bodies and centrioles are formed using distinct. J. Cell Biol. *203*, 417–425.

Thaiparambil, J.T., Eggers, C.M., and Marcus, A.I. (2012). AMPK regulates mitotic spindle orientation through phosphorylation of myosin regulatory light chain. Mol. Cell. Biol. *32*, 3203–3217.

Théry, M., Racine, V., Piel, M., Pépin, A., Dimitrov, A., Chen, Y., Sibarita, J.-B., and Bornens, M. (2006). Anisotropy of cell adhesive microenvironment governs cell internal organization and orientation of polarity. Proc. Natl. Acad. Sci. *103*,

19771–19776.

Ullrich, O., Reinsch, S., Urbe, S., Zerial, M., and Parton, R.G. (1996). Rab11 Regulates Recycling through the Pericentriolar Recycling Endosome. J. Cell Biol. *135*, 913–924.

Vasquez, R.J., Howell, B., Yvon, a M., Wadsworth, P., and Cassimeris, L. (1997). Nanomolar concentrations of nocodazole alter microtubule dynamic instability in vivo and in vitro. Mol. Biol. Cell *8*, 973–985.

Vertii, A., Hung, H.F., Hehnly, H., and Doxsey, S. (2016). Human basal body basics. Cilia *5*, 1–7.

Wakida, N.M., Botvinick, E.L., Lin, J., and Berns, M.W. (2010). An Intact Centrosome Is Required for the Maintenance of Polarization during Directional Cell Migration. *5*, e15462.

Walker, R.A., Brien, O., Pryer, K., Soboeiro, M.E., Voter, W.A., Erickson, H.P., and Salmon, E.D. (1988). Dynamic Instability of Individual Microtubules. J. Cell Biol. *107*, 1437–1448.

Westlake, C.J., Baye, L.M., Nachury, M. V, Wright, K.J., Ervin, K.E., Phu, L., Chalouni, C., Beck, J.S., Kirkpatrick, D.S., Slusarski, D.C., et al. (2011). Primary cilia membrane assembly is initiated by Rab11 and transport protein particle II (TRAPPII) complex- dependent traf fi cking of Rabin8 to the centrosome. Proc. Natl. Acad. Sci. *108*, 2759–2764.

Woodruff, J.B., Wueseke, O., Hyman, A. a, and B, P.T.R.S. (2014). Pericentriolar

material structure and dynamics. Philos. Trans. R. Soc. B Biol. Sci. *369*.

Wu, J., Misra, G., Russell, R.J., Ladd, A.J.C., Lele, T.P., and Dickinson, R.B. (2011). Effects of dynein on microtubule mechanics and centrosome positioning. Mol. Biol. Cell *22*, 4834–4841.

Yamashita, Y.M. (2009). The centrosome and asymmetric cell division. Prion *3*, 84–88.

Young, A., Dictenberg, J.B., Purohit, A., Tuft, R., and Doxsey, S.J. (2000). Cytoplasmic Dynein-mediated Assembly of Pericentrin and ✐ Tubulin onto Centrosomes □. Mol. Biol. Cell *11*, 2047–2056.

Yvon, A.-M.C., Wadsworth, P., and Jordan, M.A. (1999). Taxol suppresses dynamics of individual microtubules in living human tumor cells. Mol. Biol. Cell *10*, 947–959.

Zheng, Z., Zhu, H., Wan, Q., Liu, J., Xiao, Z., Siderovski, D.P., and Du, Q. (2010). LGN regulates mitotic spindle orientation during epithelial morphogenesis. J. Cell Biol. *189*, 275–288.

Zheng, Z., Wan, Q., Liu, J., Zhu, H., Chu, X., and Du, Q. (2013). Evidence for dynein and astral microtubule-mediated cortical release and transport of Gαi/LGN/NuMA complex in mitotic cells. Mol. Biol. Cell *24*, 901–913.

Zimmerman, W.C., Sillibourne, J., Rosa, J., and Doxsey, S.J. (2004). Mitosis-specific anchoring of gamma tubulin complexes by pericentrin controls spindle organization and mitotic entry. Mol. Biol. Cell *15*, 3642–3657.